Chapter 3:

Understanding Surface Water - Groundwater Interaction, Submarine Groundwater Discharge, and Associated Nutrient Loading in a Small Tropical Island Watershed

Abstract

Submarine groundwater discharge (SGD) provides important connectivity delivering land-based nutrients to coastal ecosystems in many oceanic islands. However, water quality management in these settings is typically focused on obvious surface waters, often ignoring SGD and nearshore groundwater-surface water interactions. In this study, we conducted a comprehensive radionuclide tracer based field investigation in tandem with watershed modeling to assess groundwater – surface water partitioning and to quantify nutrient loading from SGD and streamflow in a small embayment located in American Samoa. We used the Soil and Water Assessment Tool (SWAT) to produce water balance and nutrient loading estimates for locations, time periods, and hydrologic pathways not measured during fieldwork. Groundwater and surface water samples were analyzed for multiple tracers including 222Rn concentrations, nutrients, and nitrogen isotopes. Measurements indicated that SGD delivers a significant proportion of coastal nutrient loads, and upper-watershed baseflow delivers very little. Seepage run measurements informed a conceptual hydrogeologic model of groundwater-surface water interaction which was then used for interpreting model results. The SWAT simulated water fluxes matched flow observations well and the model simulated observed nutrient loads within an order of magnitude. The model also provided estimates of nitrogen loads in surface runoff and lateral flow, which were not measured, but together are likely to be smaller than those from SGD. By applying this integrated approach, our study demonstrates how watershed modeling can supplement limited field data to develop a more complete understanding of nutrient sources, transport, and fate in coastal watersheds with perennial streams.

Submitted to Journal of Hydrology (March 2019) as: Christopher K. Shuler, Henrietta Dulai, Olkeba T. Leta, Joseph Fackrell, Eric Welch, and Aly I. El-Kadi. Understanding Surface Water - Groundwater Interaction, Submarine Groundwater Discharge, and Associated Nutrient Loading in a Small Tropical Island

3.1 Introduction

Discharge of anthropogenic nutrients to coastal areas has the potential to significantly impact nearshore water quality and affect reef health (Bahr et al., 2015; Dulai et al., 2016). In recent decades, the effect of submarine groundwater discharge (SGD) on coastal nutrient budgets has become widely recognized (e.g., Johannes and Hearn, 1985; Dulaiova et al., 2006; Rodellas et al., 2015), and SGD has been found to be particularly significant in tropical volcanic island settings (Zektser, 2000; Moosdorf et al., 2015; Dulai et al., 2016). Nonetheless, environmental water quality management is typically focused on surface waters, often ignoring SGD. The U.S. Environmental Protection Agency's Clean Water Act (Section 303(d)) requires states and territories to establish water quality standards and Total Maximum Daily Loads (TMDLs) for nutrients in receiving waters. In many places, including the Territory of American Samoa, such standards apply only to fresh surface and open coastal waters (AS-EPA, 2013a), thereby overlooking potentially important nutrient pathways. Spatial variability in groundwater discharge directly to streams may also affect the validity of TMDL measurements, which are assumed to be from a surface water origin. Recent studies from streams (e.g., Avery et al., 2018), mangrove environments (e.g., Gleeson et al., 2013) and large tidal estuaries (e.g., Makings et al., 2014) indicate that groundwater has significant impacts on both coastal water quality and nearshore stream water quality, underscoring the importance of considering groundwater-surface water interaction when designing water quality monitoring protocols. However, accurate quantification of groundwater discharge to streams and coastlines is inherently challenging because available methods typically rely on measurements and conceptual models with high uncertainties. This underscores the need to develop an improved understanding of how land-use, groundwater, and surface water interact to deliver nutrients to the coast.

The naturally occurring noble gas radon-222 (^{222}Rn) has become one of the most widely used tracers for determining SGD rates, (e.g., Burnett and Dulaiova, 2003; Charette et al., 2007; Sadat-Noori et al., 2015) and when combined with water quality sampling, this method is widely used for estimating associated coastal nutrient fluxes (e.g., Dulaiova et al., 2010; Gleeson et al., 2013; Wang et al., 2017). Radon has also been applied successfully in stream headwaters, channels, and estuaries for investigating the magnitude and locations of groundwater-surface water interactions (e.g., Peterson et al. 2010, Gleeson et al., 2018). Groundwater becomes enriched in ^{222}Rn through prolonged contact with aquifer material, and pore-water ^{222}Rn concentrations typically reach an equilibrium between ingrowth and radioactive decay within a couple of weeks. After leaving the aquifer, dissolved ^{222}Rn has a short half-life of 3.8 days, exhibits conservative behavior through the full salinity range, and shows low concentrations in surface and ocean waters, making it an excellent tracer of recently discharged groundwater.

Predictable isotopic fractionation of nitrogen (N) in dissolved nitrate and nitrite ($\delta^{15}N_{N+N}$) has been used extensively for tracing sources of nutrients in groundwater (e.g.

Kendall and Aravena, 2000; Cole et al., 2006; Hunt, 2007), stream water (e.g. Lindau, et al., 1989), and coastal surface waters (e.g. Garrison et al., 2007; Wong et al, 2014; Wiegner, 2016; Bishop et al., 2017). Commonly referenced ranges for $\delta^{15}N$ values indicate synthetic fertilizer influenced waters have relatively low $\delta^{15}N$ values (-5 ‰ to +5 ‰), natural soil processes typically produce porewaters with intermediate $\delta^{15}N$ values (+2 ‰ to +6 ‰), and manure and human wastewater leachates generally produce higher $\delta^{15}N$ values, albeit with a wide range (+4 ‰ to+25 ‰) (Kendall and Aravena, 2000; Dailer et al. 2010; 2012; Fenech et al., 2012, Abaya et al. 2018a,b). In tropical island settings wastewater $\delta^{15}N$ values have been found to encompass almost this full range, from 5 ‰ to 23 ‰ (Bishop et al, 2017; Amato et al, 2016; Hunt and Rosa, 2009; Rogers et al, 2012).

Watershed and nutrient budget models are commonly applied to integrate diverse environmental datasets and to assess coastal water and nutrient fluxes at larger spatial and temporal resolutions (e.g. Alexander et al., 2002; Borah and Bera, 2004; Paul et al., 2017). These include the Soil & Water Assessment Tool (SWAT) (Arnold et al., 1998; Gassman et al., 2007), Gridded Surface/Subsurface Hydrologic Analysis (GSSHA) (Downer and Ogden, 2006), and Spatially Referenced Regression on Watershed Attribute (SPARROW) (Schwarz et al., 2006). The wide spatial coverage and often low development cost of models makes them useful for management agencies tasked with covering large areas that are difficult to fully characterize with field methods. However, the accuracy of model results directly relies on an appropriate conceptualization of the hydrologic system, as well as sufficient calibration and validation data to constrain uncertainty and ensure that results are accurate. Only a limited number of studies have integrated in-depth field investigations, conceptual hydrogeologic models, and distributed watershed models to characterize and assess nutrient delivery through all hydrologic pathways in small island watersheds (e.g., Oberdorfer, 2003; Michael, 2005; Gardner and Wilson, 2006; Zhu et al., 2017). To our knowledge, tropical island settings remain understudied in this regard.

Anthropogenic nutrient loading and sedimentation on American Samoan reefs have been identified as primary factors in reducing the reef's ability for recovery from increasing environmental stressors (McCook, 1999; Craig, 2009). Long-term studies of reefs on Tutuila, the territory's main island, suggest SGD is likely to be a significant explanatory variable in reef health (Houk et al., 2013; Whitall and Holst, 2015). However, prior to this study, there have been no known attempts to quantify SGD and its associated nutrient loading in American Samoa. To fill this gap, we used measurements of environmental tracers including ^{222}Rn, dissolved nutrients, and nitrogen isotopes to a trace groundwater discharge, partition baseflow and SGD nutrient flux, and explore probable nutrient sources within a small, tropical-island watershed and embayment. Field observations provided insights for informing conceptual model development and were useful for model calibration and validation. Watersheds in American Samoa provide unique settings to examine nutrient budgets on a

basin-wide scale due to small drainage areas, relatively good accessibility, and high precipitation rates that drive measurably significant water fluxes.

In this study, we hypothesize that multiple hydrologic pathways, including groundwater, surface water, and SGD all act as significant controls on coastal nutrient loading within in a small watershed located in the Territory of American Samoa. To investigate this question, we integrated a detailed geochemical field investigation with watershed-nutrient modeling in order to partition the impact of water and nutrient discharge from different hydrologic pathways. Our primary objectives for this work are to develop a better understanding of groundwater – surface water interaction in these types of watersheds and to quantify coastal nutrient loading impacts from non-point sources in Faga'alu (Fong-uh ah-loo) Watershed on the island of Tutuila.

3.2 Study Area

Faga'alu Watershed consists of a small (2.1 km^2), steep, heavily forested valley with one main perennial stream draining into Faga'alu Bay, a small arm of Pago Pago Harbor (Fig. 3.1). Geologically, the watershed is carved from dense inner-caldera basalts formed about 1.2 Mya, and the valley bottom is filled with a gently inclined wedge of terrestrial and marine alluvium that extends about 1 km upstream from the coast (Stearns, 1944). The regional scale aquifer permeability of the inter-caldera basalts is likely to be significantly lower than that of the terrestrial alluvium, based on aquifer properties of similar geologic units in Western Tutuila (Izuka et al., 2007). However, in Faga'alu the only known well is located in the alluvium, precluding direct comparison of each unit's hydrogeologic properties. Significant springs found in the inter-caldera unit indicate that it contains high-level groundwater, which is likely to be impounded by sub-surface structures, such as dikes, perching layers, or potentially faults (Davis, 1963). In the upper watershed, the soil type is primarily silty clay to clay loam Lithic Hapludolls ranging from 20–150 cm deep, and the alluvial unit is covered with a fairly deep (>150 cm) mixture of well-drained very stony silty clay loams and poorly-drained silty clay to fine sandy loams (Nakamura, 1984). Faga'alu's climate is warm and humid with year round average temperatures around 28□ C and annual rainfall between 3000 and 6000 mm/year, depending on elevation. The wet season extends from October to May and the drier season spans June to September.

In Faga'alu, anthropogenic activities have been connected to recent degradation of reef health and reduction of stream water quality, leading to its designation as a federal priority watershed management area by the United States Coral Reef Task Force (NOAA-CRCP, 2013). Both stream and coastal water quality in Faga'alu have been classified as 'impaired' since 2006 (AS-EPA, 2016) and AS-EPA coral reef monitoring suggests that Faga'alu's benthic ecosystem is one of the most impacted on the island (Houk et al., 2005). Previous studies implicate the

stream as a pathway for terrigenous sediments and excessive nutrient loads to the bay (DiDonato, 2005; Messina, 2013; Messina & Biggs, 2016). However, the role of groundwater as a hydrologic pathway for terrigenous contamination remains unconstrained. The three primary anthropogenic nutrient sources on Tutuila have been previously determined to be: (1) On-Site wastewater Disposal Systems (OSDS), (2) widespread small-scale pig farming operations, and (3) agricultural fertilizers (Falkland et al., 2002; Polidoro et al., 2016; Shuler et al., 2017); but the relative impact of each source on coastal ecosystems remains poorly understood.

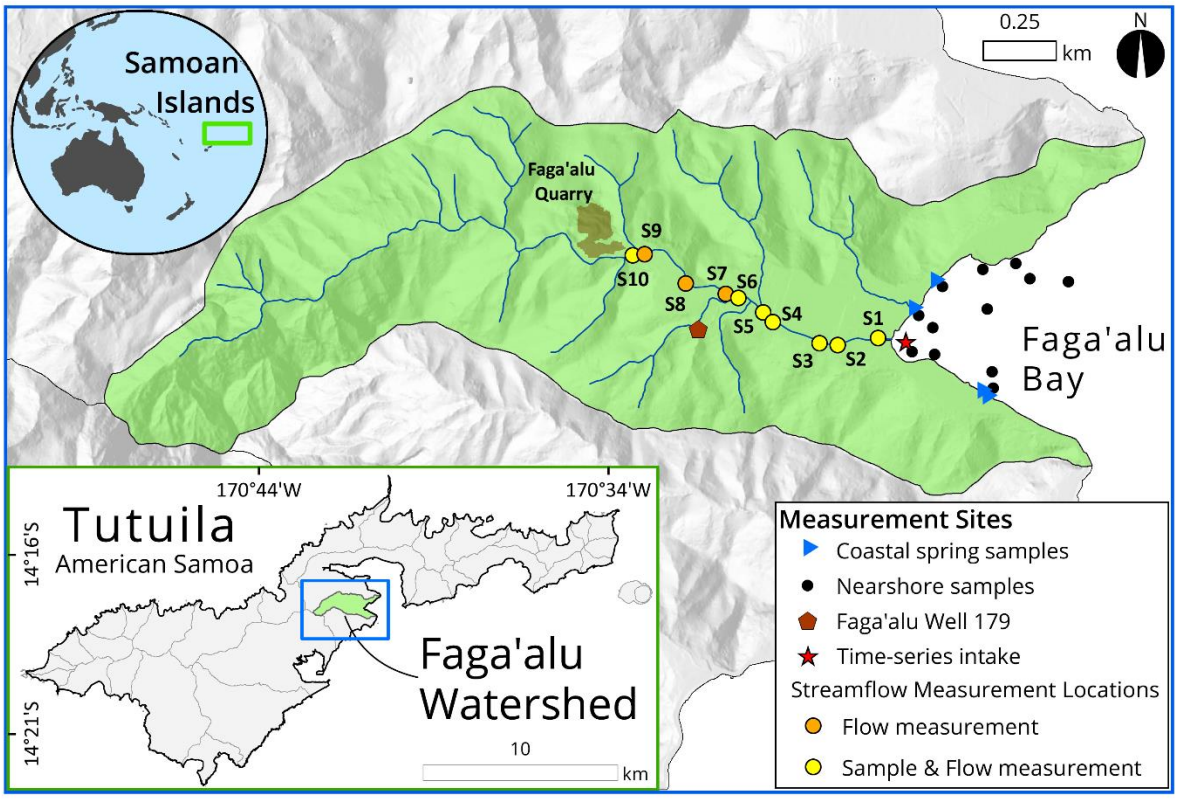

Figure 3.1: Study area and locations of sample sites in stream (colored circles), well (pentagon), coastal springs (triangles), and nearshore waters (black circles). Flow measurements were taken at all stream sites and yellow circles indicate where water samples were taken as well. The seepage run focused on the lower reach of Faga'alu Stream (below the quarry) as this reach encompassed the majority of human development within the valley.

3.3 Methods

3.3.1 Water Sampling and Stream Gauging Methods

We collected groundwater, coastal water, and stream water samples throughout a weeklong sampling campaign in the dry season of 2014 during a period with no significant rainfall. This included a longitudinal sampling and measurement transect up Faga'alu stream, hereafter referred to as a seepage run (Rosenberry and LaBaugh, 2008), which we conducted during a single 24-hour period through the lower 1 km stream section. During the seepage run, we measured streamflow at ten separate locations with a Price-type Pygmy Current Meter and the velocity-area-method (Turnipseed and Sauer, 2010) and sampled stream water at seven of those locations. During a boat-based coastal water survey (see section 3.2.2), we collected coastal water samples from Faga'alu Bay one day after the seepage run. We identified three areas along the shoreline of the bay with brackish coastal springs, and sampled these twice each at low tide throughout the week. We also sampled the only production well in the valley (Well #179). All sampling locations are shown on Fig. 3.1. To verify the seepage run results, we conducted a second seepage run on August 10th, 2016, and measured streamflow and dissolved ^{222}Rn concentrations (but not nutrients or other parameters) at many of the same sites as in 2014. To reduce measurement uncertainty, streamflow for the second seepage run was measured with a SonTek FlowTracker Handheld Acoustic Doppler Velocimeter, which has a higher velocity resolution and accuracy than the Pygmy meter we used in 2014. Sampling and analysis for ^{222}Rn concentrations was performed in the same way as was done in 2014.

For all nutrient samples, we also collected in situ temperature, salinity, pH, and dissolved oxygen data with a YSI multiparameter sonde (6600V2-4 model). Nutrient and isotope samples were collected in acid washed 60 ml HDPE bottles triple-rinsed with sample water before filling. Nutrient samples were kept refrigerated, whereas N-isotope samples were frozen until analysis. All nutrient and isotope samples were filtered through 0.45 μm capsule filters, thus all measured nutrient concentrations and comparable modeled nitrogen concentrations reported here refer to dissolved species unless the particulate fraction is specifically indicated. We collected grab samples for ^{222}Rn in 250-ml glass bottles with no headspace and analyzed them the same day as collection with a RAD H_2O radon in water analyzer, manufactured by Durridge Inc. (Billerica MA, USA). Because of ^{222}Rn's short half-life (3.8 days), ^{222}Rn grab sample values were decay corrected to the time of collection.

We analyzed all water samples for dissolved nutrients including nitrate and nitrite (N+N), ammonium (NH_4^+), phosphate (PO_4^{3-}), silicate (Si), total dissolved nitrogen (TDN), total dissolved phosphorus (TDP), dissolved ^{222}Rn concentration, and nitrogen isotope ($\delta^{15}N_{(N+N)}$) values of N+N in samples having > 1 μmol/L of N+N. The only exceptions were samples collected in 2016, which were only analyzed for ^{222}Rn concentrations. Nutrient samples were analyzed within two weeks of collection at the University of Hawaii School of

Ocean and Earth Science and Technology (SOEST) Laboratory for Analytical Biogeochemistry using the methods described in Armstrong et al. (1967) and Grasshoff et al. (2007). Nitrogen isotope samples were measured within 4 months of collection at the University of Hawaii's Stable Isotope Biogeochemistry Lab using the denitrifier method of Sigman et al. (2001). Isotopic results are expressed here in per mil (‰) notation relative to the isotopic reference standard of AIR.

Since coastal groundwater is composed of both oceanic and fresh water, all reported nutrient concentrations for coastal springs were normalized to the fresh groundwater end-member salinity of 0.16, as measured at Well 179. This was done with an un-mixing calculation (e.g., Hunt and Rosa, 2009) that assumed conservative nutrient behavior during mixing and was based on an oceanic end member from Tutuila. This calculation allowed the derivation of nutrient fluxes solely contributed by fresh groundwater. We collected duplicate samples at five locations and analytical uncertainty was assessed using the relative percent difference (RPD) method, which is defined as the absolute value of the difference between two duplicates, expressed as a percentage of their mean. Average RPD was 1.4% for N+N, 0.5% for Si, 0.6% for PO_4^{3-}, 2.4% for NH_4^+, 0.8% for TDN, 1.9% for TDP, and 6.8% for $\delta^{15}N_{(N+N)}$.

3.3.2 Radon-Based SGD Measurement

Dissolved ^{222}Rn was used as a groundwater tracer in a temporally and spatially distributed non-steady-state radon flux model to calculate bay-wide SGD rates following the methods of Burnett & Dulaiova (2003) and Dulaiova et al. (2010). We assessed temporal (tide-dependent) variability with a time-series of ^{222}Rn measurements taken from a fixed nearshore location over a 48-hour period. This was coupled with a coastal water survey to assess spatial variation in ^{222}Rn throughout the inner bay. For both the time-series and survey, ^{222}Rn concentrations were measured by pumping surface water through an air-water exchanger connected to a radon-in-air monitor (RAD AQUA, Durridge Inc.). To obtain bay-wide SGD fluxes, we scaled up the tidally-averaged SGD flux from the stationary time-series to account for the additional SGD flux observed during the coastal survey in locations adjacent to the time-series location, as described below.

3.3.2.1 Stationary ^{222}Rn Time-Series

The ^{222}Rn time-series instrument package used a peristaltic pump that pumped surface water from the bay to an instream flow cell (with no headspace) attached to the YSI 6600-series sonde that continuously logged water salinity and temperature. The inlet hose for the pump was connected to a moored float located at a stationary point in the bay about 50 m away from the stream mouth (Fig. 3.1). After passing through the YSI, water flowed into an air-water-exchanger where ^{222}Rn gas was extracted and pumped to the RAD7. Tidal height

was measured by a pressure transducer placed on the seafloor at the float anchor. We deployed the instrumentation for about 48 hours and the RAD7 was set to integrate measurements of ^{222}Rn activity every 30 minutes. Typically, SGD manifests as a fresh or brackish plume that overlies denser seawater. We measured plume thickness at low tide by manually conducting salinity depth profiles at the water intake, and this plume thickness was used for volumetric calculations in the ^{222}Rn mass-balance model. Change in plume thickness due to tidal dilution was calculated by subtracting the thickness of the underlying salt-water layer from the total depth of the water column.

3.3.2.2 Coastal Water Survey

We performed the coastal water survey once the time-series was finished, during a 3-hour period bracketing low tide. We transferred the time-series instrument platform to a small boat and rowed throughout the bay while the air-water exchanger was supplied with surface water from a bilge pump tethered to the hull of the boat. The RAD7 was set to integrate ^{222}Rn activity every 5 minutes and data was resampled to one minute intervals yielding a total of 205 points available for interpolation. During the survey, three distinct plumes of SGD were detected as low salinity and high ^{222}Rn anomalies. We refer to these plumes as the southern, central, and northern plumes. During analysis, the surface area and geometry of each plume was determined by nearest neighbor interpolation of measurement points and contouring of the resultant ^{222}Rn activity surface. Boundaries for each of the three plumes were defined as the ^{222}Rn-isoline representing the mid-point of the range of measured activities (3.25 dpm/L). We defined the bottom boundary of each plume to be the salinity 28 isohaline, as indicated by salinity depth profiles that we took periodically during the survey; or if salinity was consistent throughout the whole water column, the full water depth was used as the plume thickness. Note that the time-series measurement described in section 3.2.1 was performed at a location that fell inside of the central plume. Additionally, during the survey, coastal water samples were collected for analysis in the same manner as stream and groundwater samples.

3.3.2.3 SGD Flux Scaling, Fresh and Recirculated Fractions

The ^{222}Rn flux model of Dulaiova et al. (2010) was used to calculate SGD fluxes for both survey and time-series data. The model uses a mass-balance approach that relies on accounting for ^{222}Rn losses and additions from local and offshore processes that are not related to SGD. We assumed that ambient ^{222}Rn activities from oceanic or atmospheric sources were comparable to those found in the Hawaiian Islands, and used an ambient ^{222}Rn activity of 0.03 dpm/L (Kelly, 2012), a local excess ^{222}Rn activity of 0.08 dpm/L supported by in situ ^{226}Ra (Street et al., 2008), and an offshore ^{222}Rn activity of 0.087 dpm/L, derived from the offshore ^{226}Ra (Fröllje et al., 2016). We assumed residence time of SGD affected-groundwater

within Faga'alu's inner bay to be 12.2 hours, the length of one tidal cycle, which is within the ranges of published residence times from water circulation studies of Faga'alu (Storlazzi et al., 2014; Vetter and Vargas-Angel, 2014). Hourly measurements of local wind speed and air temperature were obtained from the American Samoa Observatory NOAA Earth System Research Laboratory (ESRL) weather station at Cape Matatula. To assess the SGD end-member composition, we collected groundwater samples from the only well in the valley and from four coastal spring locations at low tide. The ^{222}Rn activity measured in coastal springs and the well showed a linear mixing relationship with salinity (Appendix C, Fig. C1), which suggests that while seawater recirculation does occur, the nearshore reef substrate or the re-infiltrated coastal water does not add a significant quantity of ^{222}Rn to groundwater during this process; likely because circulation is rapid and recirculated seawater does not spend enough time in the subsurface to collect measurable radon. The linearity of this relationship also indicates the fresh coastal spring ^{222}Rn end-members (when corrected for dilution by seawater) are quite consistent with the ^{222}Rn activity measured at Well 179. Therefore, the ^{222}Rn concertation from the well was used as the groundwater end member for SGD calculations.

The time-series calculations provided a temporally-integrated SGD rate, but for the central plume only, as this was where the water intake was located. On the other hand, the coastal water survey provided spatially distributed SGD rates, which allowed for the identification of three distinctive SGD plumes, but only as a snapshot in time. Therefore, to calculate temporally integrated SGD flux to the whole bay, the ratios of survey-measured SGD rates in the northern and southern plumes to the survey-measured SGD rate in the central plume were used as scaling factors to upscale the time-series derived, temporally-averaged SGD flux to include the other two plumes. Some limitations of this approach included needing to make the simplifying assumptions that tidal variation in the central plume was representative of the other two plumes, that SGD only discharged from the three identified plumes, and that the relative magnitudes of discharge from each plume stay consistent over time. These limitations could be addressed by replicating the survey at different times or repeating the time-series in different locations. However, due to the significant amount of time required for just one time-series and survey, we were unable to replicate the approach at a different time.

3.3.3 Watershed and Land-Use Modeling

For watershed modeling, we selected the SWAT model, which is a physically-based, semi-distributed, watershed scale, ecohydrological model (Arnold et al., 1998). The model served as a framework for integrating a diverse spread of field data and for estimating transient magnitudes of flow and nutrient flux through different hydrologic pathways (water budget components), such as surface runoff, lateral flow (i.e., subsurface stormflow), and baseflow at different spatial and temporal scales. The wide applicability of SWAT under

various conditions and to different environmental problems has been demonstrated worldwide (Gassman et al., 2007 and 2014).

The SWAT model development was based on the following datasets:

- A 3x3 m Digital Elevation Model (DEM) from the National Geophysical Data Center ([dataset] NGDC, 2013) and obtained from NOAA Ocean and Coastal Services Center.
- 1:24,000 scale soil maps from the Natural Resources Conservation Service - Soil Survey Geographic (SSURGO) database.
- A 2.4 x 2.4 m 2010 land-use map from the Coastal Change Analysis Program (C-CAP).
- Anthropogenic dissolved inorganic nitrogen (DIN) source locations and loading rates as detailed below.

Daily rainfall and streamflow were measured and provided for this study by A.M. Messina (2016 personal communication, with supporting methodology documented in (Messina, 2016)) at two sites within the Faga'alu Watershed for the period 2012 to 2014. Daily wind speed, relative humidity, and maximum and minimum temperatures were only available at one of these sites. Solar radiation was measured at the nearby American Samoa Community College ([Dataset] ASCC, 2018) and additional relative humidity data were obtained from the NOAA- Earth System Research Laboratory weather station. The watershed was divided into 26 sub-basins and 403 hydrological response units (HRUs), with zero threshold values for land-use, soil, and slope classes. The model simulation was run for the period of 2005 to 2014.

Nitrogen budget modeling was handled in SWAT by populating the model with locations and estimates of anthropogenic N sources, specifically agricultural applications, piggery waste, and household wastewater discharged via On-Site Disposal Systems (OSDS). Agricultural DIN was loaded as a fertilizer application, pig waste was simulated as a manure application, and OSDS leachate was simulated using SWAT's biozone algorithm module for OSDS simulation (Jeong et al., 2011). We obtained piggery locations and stock numbers from an AS-EPA piggery census GIS-dataset ([Dataset] Zennaro, 2007) provided by AS-EPA, and agricultural land-use areas were taken from the C-CAP land-use map mentioned above. Because no OSDS survey data is available for the Faga'alu area, we indirectly determined the locations of OSDS units, following Shuler et al. (2017), by taking all building locations, and geospatially subtracting those within 10 m of a sewer main or connection as indicated by wastewater as-built diagrams supplied by the American Samoa Power Authority (ASPA). The remaining buildings were assumed to be connected to an OSDS unit. Maps of input datasets used in the SWAT model are shown in (Fig. 3.2). We based the N-loading rate for pig manure on a reported value of 14 kg of N/pig/year (AS-EPA, 2013b), the agriculture loading rate was based on the synthetic fertilizer application rate of 2.81 kg-N/ha of arable land/year as

reported in Samoa ([Dataset] The World Bank, 2015). The loading rate for OSDS units was estimated to be 18.2 kg-N/unit/year, which was based on a published per capita N loading rate for failing septic systems (TCE, 2005) and the average number of occupants in American Samoan households (AS-DOC, 2013). Because most of the OSDS units in American Samoa are cesspools, we considered failing septic systems to be the best approximation for these types of units. Natural nitrogen cycling processes were automatically handled in SWAT based on the default ecological nitrogen production rates from each assigned land-use type.

Because SWAT's ecological nitrogen cycling processes also act on anthropogenic nitrogen sources, the relationship between anthropogenic N input and N discharge due to each source is non-linear. To get around this issue we ran three different model scenarios, each with one of the three individual anthropogenic N source removed as an N input. In this way, source-specific loading rates to each hydrologic pathway could be calculated as the difference between the scenario and base-case N discharge to each pathway. A forth scenario with all anthropogenic sources removed was also run to determine how much N is discharged when accounting for natural N cycling only.

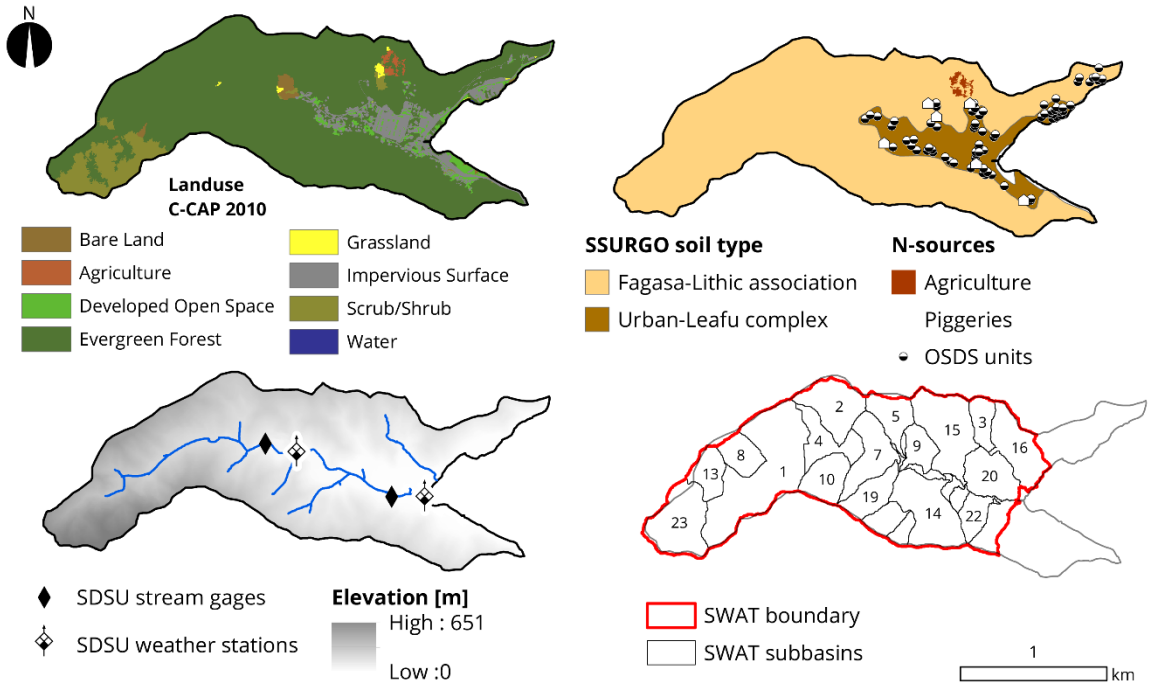

Figure 3.2: Input datasets used in SWAT model. These included (clockwise from top left) (1) land-use type, (2) soil type, with locations of N sources, (3) model boundaries, and (4) land surface elevation, and locations of weather and streamflow monitoring points.

3.4. Results

3.4.1 Conceptual Hydrogeologic Model

By integrating information about the study area's underlying geology with geochemical and physical measurements, we were able to develop a simple conceptual model of Faga'alu's groundwater-surface water interaction during baseflow conditions (Fig. 3.3). In its upper reaches, dense trachyte and older lava flows underlie the stream (Stearns, 1944), and dikes may also serve to impound groundwater in the shallow subsurface (Davis, 1963). On basaltic islands, dikes or low-permeability structures commonly impound groundwater at high-elevations (Takasaki and Mink, 1985). On a hike to the upper portion of the watershed, we observed numerous springs and small tributaries, indicating a general net transfer of groundwater to surface water in this area. Davis (1963) also documents the significance of springs in the upper Faga'alu watershed based on their historical water usage. Although this spring water is expected to be enriched in ^{222}Rn upon discharge, numerous waterfalls and high turbulence throughout the upper-reaches promote evasion, which significantly reduces ^{222}Rn concentrations as the water flows downhill. At Faga'alu Quarry, which lies at the upper edge of Faga'alu Village, the stream channel slope declines, and the lithology changes to an alluvial valley-fill, likely with higher permeability (Izuka et al., 2007). In the portion of the stream underlain by alluvial-fill, we observed low ^{222}Rn levels and declining streamflow (except where two very small tributaries between sites S5 and S6 were seen to contribute water to the main branch), suggesting the stream is losing water to the aquifer in this reach (see section 4.2 below). Once the stream nears the coast, streamflow, ^{222}Rn, and nutrient values spike, indicating this is an area of groundwater discharge, likely from a basal-lens aquifer within the alluvium. When corrected for mixing with high-level baseflow, the nutrient signature of this basal-lens baseflow is a fairly close match to the composition of salinity unmixed coastal spring discharge, suggesting that both of these water sources originate from the same nearshore aquifer.

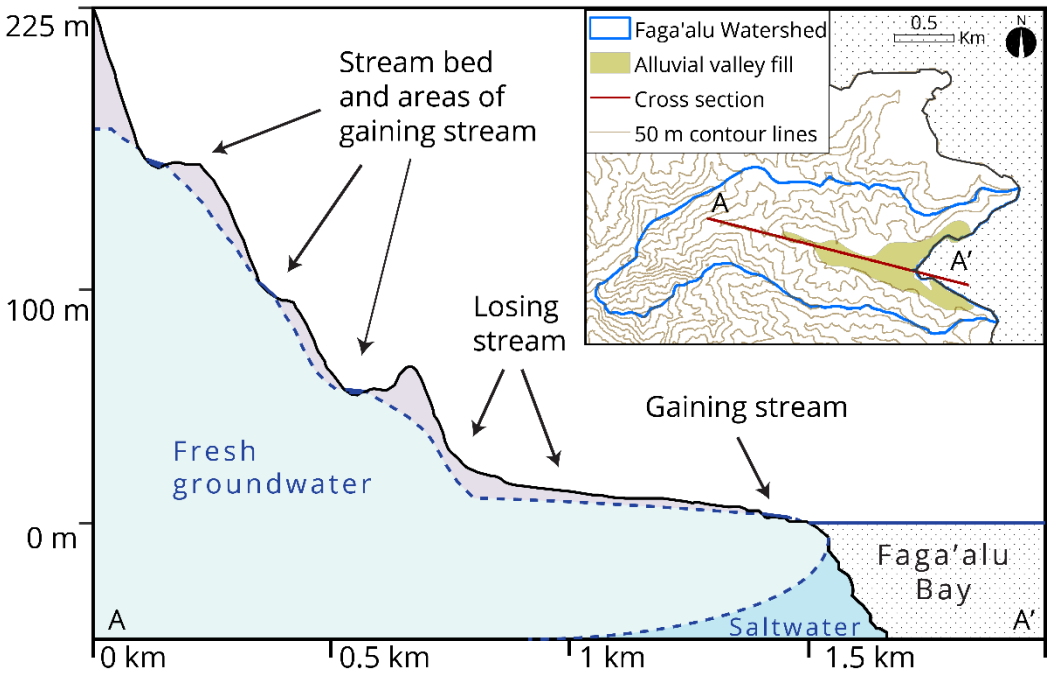

Figure 3.3: Conceptual schematic cross-section of groundwater-surface water interaction in Faga'alu watershed, based on geological information, geochemical data, and physical observations. The stream gains from high-level groundwater in its upper section and upon reaching the more permeable alluvial fill on the valley floor, begins to slowly lose water. The stream again intersects the water table near the coast where basal-lens groundwater discharges to the nearshore stream reach. Upper right panel shows map view of the valley topography and extent of alluvial valley fill.

3.4.2 Characterization of Baseflow Components

Dissolved ^{222}Rn concentrations in the stream were generally low (6-10 dpm/L), except at the two sites nearest the coast (sites S1 and S2), where values increased up to 42 dpm/L. Coincident with increased ^{222}Rn concentrations between the uppermost (S10) and lowermost (S1) sites, were increases in flow from 2,700 to 3,524 m^3/d, DIN concentrations from 4 to 12 µmol/L, and $\delta^{15}N_{(N+N)}$ values from 4.5 to 11.5‰ (Fig. 3.4). The simultaneous increase in $\delta^{15}N_{(N+N)}$ and DIN input suggests a portion of this DIN may be derived from human or animal waste, which both produce nitrogen with an elevated $\delta^{15}N$ signature (Kendall, 1998). Because there were no observed surface tributaries above the lowest stream sampling sites, the coincident increases in water, nutrients, and ^{222}Rn indicates the stream receives significant basal groundwater discharge just before exiting to the bay. The 2016 seepage run showed almost the exact same pattern, although ^{222}Rn concentrations through the whole stream and particularly near the stream mouth were observed to be higher (up to 122 dpm/L).

Based on these observations, baseflow discharge to the bay can be viewed as a mixture of two distinct components, (1) baseflow sourced from high-level groundwater (Davis, 1963) (here referred to as high-level baseflow) and (2) baseflow sourced from basal-lens groundwater (here referred to as basal-lens baseflow). We estimated the fraction of high-level

baseflow (f_S) to basal-lens baseflow (f_{GW}) discharged in the stream estuary with a simple two end-member mixing model applied to ^{222}Rn concentrations using the groundwater end member and surface water from the upper portion of the stream (as measured at site S3):

$$f_{GW} + f_S = 1 \quad (1)$$

$$f_S = \frac{C_{mix} - C_{GW}}{C_S - C_{GW}} \quad (2)$$

Where (C_S) is the average concentration of ^{222}Rn measured at site S3, (C_{GW}) is the ^{222}Rn concentration in groundwater at production well #179, and (C_{mix}) is the mixed sample ^{222}Rn concentration measured at the most coastal stream site, S1. Results from 2014 data indicate stream water at site S1 was composed of 67% high-level baseflow (2,368 m^3/d) and 33% (1,156 m^3/d) recently discharged basal-lens baseflow. Although this calculation assumes conservative radon behavior (no radioactive decay and no atmospheric evasion over the timescale of the water flow), the estimate compares reasonably well to the flow increase as directly measured by stream gauging, which showed an addition of 957 m^3/d, or an additional 27% between site S3 and site S1 (Table 3.1). The 2016 seepage run was conducted at baseflow conditions as well. Total baseflow discharge at the lowest stream site in 2016 was 3,629 m^3/d. When 2016 seepage run data was substituted into equations (1) and (2), ^{222}Rn based partitioning of streamflow between high-level and basal-lens baseflow was very comparable to the 2014 results. The 2016 calculation indicated 66% of the stream's flow (2,412 m^3/d) originated from the high-level fraction and 34% (1,217 m^3/d) originated from the basal-lens. The 2016 streamflow measurements show a flow increase of 37% or an additional 1,339 m^3/d between the lowest site (site S1) and flow at site S3. Because we did not take nutrient measurements or calculate SGD fluxes in 2016, we present the 2016 seepage run data as validation for streamflow partitioning only. For nutrient flux calculations we only used data from 2014.

We calculated baseflow nutrient flux rates by multiplying the respective measured flow rates by the nutrient concentrations observed in each baseflow component (high-level and basal-lens baseflow). Total baseflow loading of DIN and PO_4^{3-} to the bay were estimated to be 0.72 ± 0.05 and 0.38 ± 0.03 kg/d, respectively. When partitioned with equations (1) and (2), basal-lens baseflow was estimated to have delivered 0.47 ± 0.05 kg-DIN/d and 0.22 ± 0.02 kg- PO_4^{3-} /d, whereas only 0.25 ± 0.03 kg- DIN/d and 0.16 ± 0.02 kg- PO_4^{3-}/d were delivered by high-level baseflow (Table 3.2).

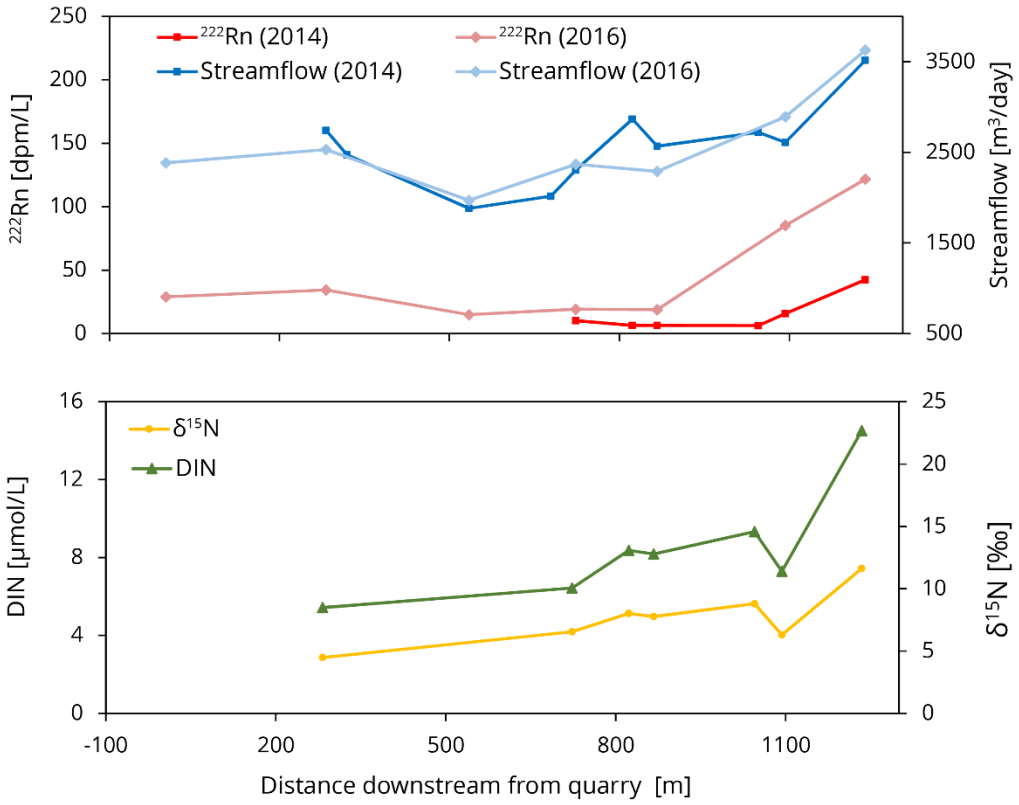

Figure 3.4: Physical (streamflow) and geochemical (^{222}Rn, DIN, and δ^{15}N) measurements from sampling points along seepage runs. The stream mouth, where the stream discharges into the bay, is located 1,250 m downstream from Faga'alu quarry, which marks the upper boundary of the lower reach of Faga'alu stream. Streamflow measurement uncertainty was not assessed, but was assumed to be 10 % of the measurement value. Note that for validation purposes, the same seepage run was reproduced in August 2016. Streamflow and ^{222}Rn data from both 2014 and 2016 seepage runs are shown in top graph. The 2016 data is shown for validation only; all calculations were performed with 2014 data.

3.4.3 SGD Rates and Nutrient Fluxes

3.4.3.1 Time-Series SGD Fluxes

During the stationary time-series, ^{222}Rn concentrations at the intake point averaged 4.8 dpm/L (range of 2.9 to 8.2 dpm/L), salinities averaged 26.9 (range of 22.3 to 33.1), and the thickness of the SGD-affected brackish plume averaged 38 cm (range of 7 to 70 cm). While the highest ^{222}Rn concentrations and the lowest salinities generally occurred at low-tide, as expected, a continuous input of higher ^{222}Rn and lower salinity water from the nearby stream mouth was also detectable in the time-series data. Conversion of ^{222}Rn concentrations to SGD fluxes with the transient radon balance model yielded an average fresh SGD rate of 2959 ± 891 m^3/d to the central plume where the intake was located. However, because the time-series measurement was taken just outside of the stream mouth, the time series and survey points

near this area were actually detecting a mixture of ^{222}Rn from coastal SGD and recently discharged basal-lens baseflow from the nearshore tidally-affected part of the stream. Subtracting the basal-lens baseflow fraction (1,156 ± 117 m^3/d) as calculated in section 4.2, left an estimated SGD rate of 1,803 ± 891 m^3/d as groundwater coming from the coastal portion of the bay only. This does assume that most or all of the ^{222}Rn from high-level baseflow has evaded by the time it reaches the coast, which if not, would bias the coastal SGD fraction of the total measured SGD to be a slight overestimate. Note that uncertainties associated with SGD fluxes represent the standard deviation of the temporal variation in discharge as this value is typically significantly larger than uncertainty propagated from individual model input parameters.

3.4.3.2 Spatial Distribution of SGD from Coastal Survey Measurements

The coastal water survey revealed three distinct groundwater discharge zones, or plumes, one each on the northern, central, and southern portions of the coastline (Fig. 3.5). We found the highest ^{222}Rn concentrations, up to 7.4 dpm/L, and thus SGD fluxes with an average of 2,623 ± 1,653 m^3/d, in the central plume, which was centered just to the south of the stream outlet. The southern plume had the lowest ^{222}Rn concentrations and SGD fluxes, up to 4.7 dpm/L and average of 266 ± 138 m^3/d, respectively, with the northern plume having ^{222}Rn concentrations up to 5.0 dpm/L and SGD fluxes averaging 846 ± 78 m^3/d.

3.4.3.3 Total SGD and Nutrient Flux Scaling with Coastal Survey Data

The time-series measurement provided critical information about temporal variability in SGD rates, but only for discharge to the central plume. Therefore, to calculate tidally-integrated average fresh SGD fluxes to the whole bay, the time-series measured discharge was upscaled to include discharge from the northern and southern plumes as well, using the spatially distributed SGD information from the survey as described in section 3.2.3. Calculated scaling factors were 0.10 for the southern plume and 0.32 for the northern plume, or in other words, SGD rates measured during the survey showed the southern and northern plumes discharged 10 % and 32 %, respectively, of the central plume's SGD rate. Bay wide SGD flux was calculated by multiplying the scaling factors by the time-series derived tidally-averaged SGD flux for each plume then summing the results of all three plumes. Multiplying these factors by the central plume's true SGD rate (1,803 ± 891 m^3/d) and summing flux from all three plumes yielded a SGD rate of 2,587 ± 899 m^3/d to the whole inner-bay.

We calculated daily nutrient fluxes from SGD by multiplying coastal discharge rates by the average of salinity-unmixed, coastal-spring nutrient concentrations (Table 3.1). Salinity unmixing for coastal springs was performed with a standard solute unmixing calculation (Hunt and Rosa, 2009) based on the salinity and nutrient composition of a local oceanic end

member sample and an assumed freshwater salinity of 0.1. Fluxes were calculated to be 1.76 + 1.28 kg-DIN/d and 0.49 + 0.31 kg-PO_4^{3-}/d (Table 3.2). Nutrient flux uncertainties were propagated from uncertainties in water discharge and nutrient concentration values.

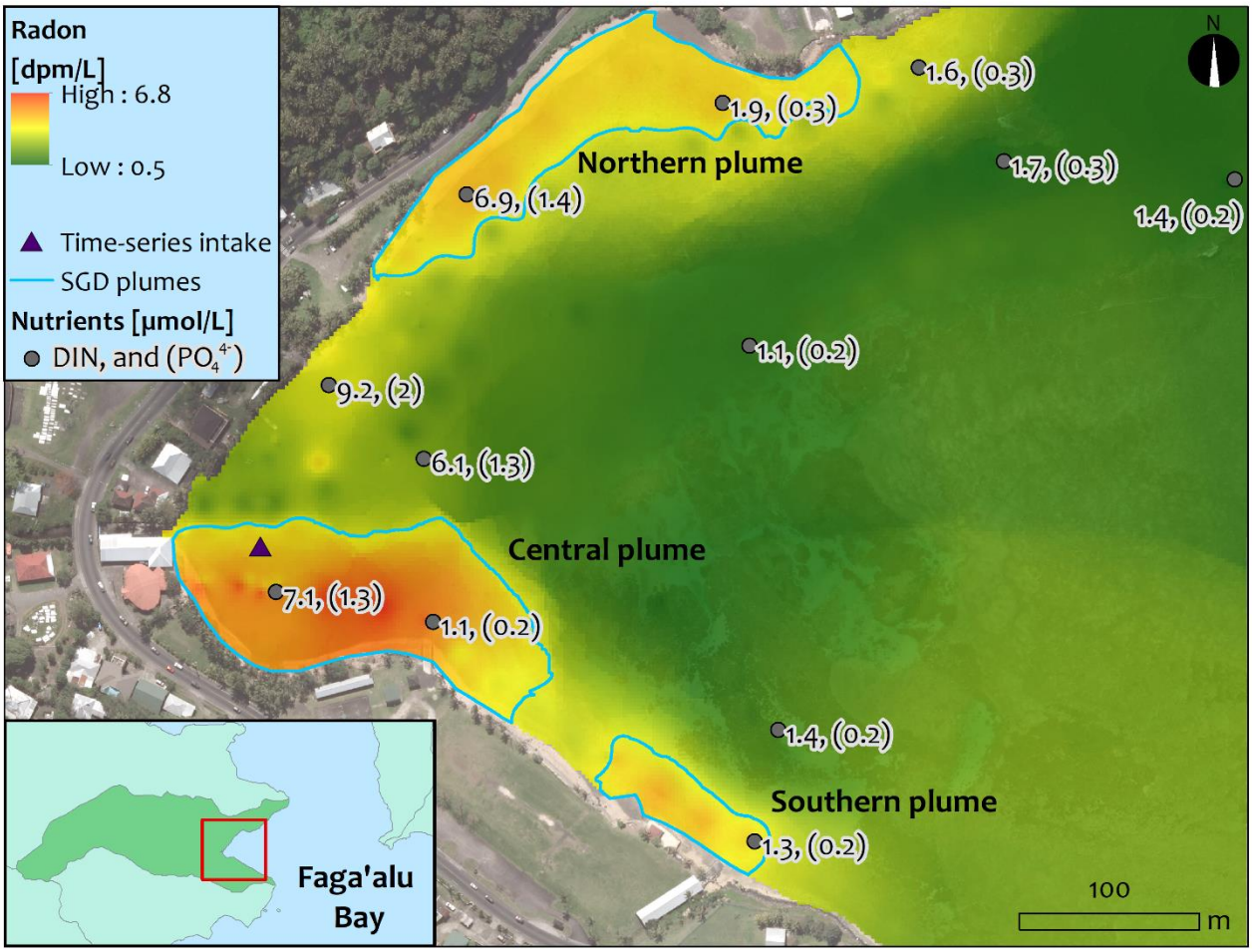

Figure 3.5: Results from coastal radon survey and surface water nutrient sampling. Dissolved radon concentrations are higher near the coast, indicating areas of groundwater discharge. Blue lines indicate defined boundaries of groundwater plumes, based on ^{222}Rn iso-lines of 3.5 dpm/L. Water sample locations (grey dots) and concentrations of DIN (first number) and PO_4^{3-} (second number inside parentheses) are also shown in µmol/L.

Table 3.1: Measured nutrient and tracer concentrations in stream (S), well (W), and salinity unmixed samples from coastal springs (Csp)

Sample name	Latitude (°South)	Longitude (°West)	Salinity (PSU)	DO (mg/L)	^{222}Rn (dpm/L)	N+N (µM)	PO_4^{3-} (µM)	SiO_4^{4-} (µM)	NH_4^+ (µM)	DIN (µM)	Total N (µM)	Total P (µM)	$\delta^{15}N$ (‰)
S1	14.29131	170.68340	0.2	6.6	42.5	12.5	3.5	522	2.00	14.5	19.7	3.4	11.61
S2	14.29153	170.68465	0.1	8.0	15.7	7.2	3.1	518	0.10	7.3	11.1	2.9	6.30
S3	14.29147	170.68521	0.1	7.6	6.3	9.1	2.9	530	0.27	9.4	14.4	2.9	8.79
S4	14.29082	170.68665	0.1	7.6	6.4	7.9	3.1	530	0.24	8.1	12.7	3.4	7.76
S5	14.29053	170.68694	0.1	7.6	6.4	7.9	3.6	519	0.41	8.3	12.7	3.4	8.01
S6	14.29008	170.68771	0.1	7.9	10.1	6.2	2.8	499	0.21	6.4	9.4	2.6	6.53
S10	14.28877	170.69096	0.1	8.0	-	5.4	2.4	502	0.03	5.4	7.8	2.3	4.47
Csp1	14.29173	170.68298	(9.6)*	0.3	1.3	5.3	3.3	197	10.9	16.2	24.3	3.3	7.47
Csp2	14.29046	170.68234	(8.1)*	0.9	62.3	0.0	8.7	299	14.1	14.1	17.7	7.9	
Csp3	14.28960	170.68167	(4.7)*	6.0	101	65.9	4.3	522	0.00	65.9	60.9	4.1	7.09
Csp4	14.29316	170.68008	(26.7)*	2.5	7.5	39.7	4.1	586	1.49	41.2	54.7	3.5	5.50
Csp5	14.29315	170.68008	(26.2)*	0.7	1.2	8.2	7.5	453	21.5	29.7	51.7	6.5	-
W179	14.29092	170.68910	0.2	0.5	124.2	8.3	8.1	632.0	2.93	11.2	13.6	8.0	5.41
Bay1	14.29180	170.68167	34.8	9.3	6.9	0.5	0.2	3.4	0.58	1.1	5.3	0.4	-
Bay2	14.29290	170.68001	34.7	9.3	3.4	0.7	0.2	7.0	0.63	1.3	5.4	0.4	-
Bay3	14.29234	170.67989	34.9	7.7	1.1	1.0	0.2	1.1	0.41	1.4	5.3	0.4	-
Bay4	14.29041	170.68004	34.6	8.5	0.4	0.6	0.2	7.0	0.47	1.1	6.1	0.5	-
Bay5	14.28957	170.67754	34.9	7.8	0.1	1.0	0.2	3.5	0.41	1.4	5.2	0.5	8.17
Bay6	14.28948	170.67873	34.7	7.9	0.3	1.3	0.3	4.0	0.45	1.8	9.4	0.5	8.56
Bay7	14.29098	170.68172	27.2	7.6	2.7	5.1	1.3	149	1.00	6.1	10.2	1.4	-
Bay8	14.29061	170.68221	16.3	7.1	3.1	7.6	2.0	240	1.56	9.2	13.8	2.0	8.76
Bay9	14.28965	170.68150	19.4	7.1	4.5	5.9	1.4	161	1.06	7.0	11.0	1.4	9.27
Bay10	14.28919	170.68018	31.4	7.0	4.1	1.3	0.3	3.7	0.65	2.0	6.0	0.5	-
Bay11	14.28901	170.67917	34.8	6.2	3.1	1.5	0.3	2.7	0.15	1.7	5.2	0.5	8.62

*Salinities in parentheses are original salinity prior to unmixing from seawater, unmixing was performed to a freshwater salinity of 0.1. Nutrient values in Csp. Samples represent fresh endmember values. Note DIN concentrations equal the sum of N+N and NH_4^+.

3.4.4 Nearshore Water Quality

In Faga'alu's coastal waters, levels of DIN (1.1 to 9.2 µmol/L) and PO_4^{3-} (0.2 to 2.0 µmol/L) in samples taken near to the shore were higher than those found in those samples farther offshore (1.1 to 1.7 µmol -DIN/L) and (0.2 to 0.3 µmol - PO_4^{3-}/L) indicating local terrestrial nutrient sources have a detectable impact on the bay's water quality (Fig. 3.5). Typically N:P ratios in oceanic waters are near 16:1. However, N:P ratios in Faga'alu's baseflow and SGD are for the most part, disproportionately lower, averaging around 6:1. In Faga'alu's coastal waters, ratios ranged between 7:1 to 20:1 and averaged 12:1 suggesting nitrogen limiting conditions. This shows that SGD not only has an impact on the amount of N and P in the bay but also on the balance of these nutrients, which can have implications for biologic processes that control factors such as eutrophication. Within the bay, nutrient concentrations are elevated in the northern relative to the southern bay (Fig. 3.5), which is likely caused by circulation within the bay (Storlazzi et al., 2018) as well as heterogeneity in the spatial distribution of SGD. The northern and central plumes show discharge rates that are 5 and 10 times higher than the southern plume, respectively, and the persistent clockwise circulating current (Storlazzi et al., 2014) would be expected to transport stream water and its associated nutrient load to the north rather than to the south.

3.4.5 SWAT Model Results

3.4.5.1 Model Calibration

For managing the calibration process, we used the SWAT Calibration and Uncertainty Program (SWAT-CUP) (Abbaspour, 2014) with the sequential uncertainty fitting (SUFI-2) method of Abbaspour, et al. (2007). We calibrated the hydrologic portion of model using daily streamflow observations for the period 2012 to 2014 from two sites on lower Faga'alu Stream. The deep-aquifer partitioning coefficient (RCHRG_DP) was also manually adjusted to match measured SGD as well as possible (see section 4.5.2). The first seven years of the model simulation period (2005-2011) were assigned as model warm up, while the period from 2012 to 2013 was used for calibration. We used the year 2014 as a validation period. The temporal evolution of observed daily streamflow hydrographs was well reproduced by SWAT with a Nash-Sutcliffe Efficiency (NSE) (Nash and Sutcliffe, 1970) of 0.65 to 0.86 for both calibration and validation periods, indicating the ability of the model to simulate daily stream flow reasonably well (Fig. 3.6a). Considering the streamflow simulation uncertainty, 57% to 87% of the observations were bracketed at the NSE 95% confidence interval (CI) for both the calibration and validation periods.

We based calibration for the nutrient flux portion of the SWAT model on a set of twenty NO_3^- and NH_4^+ nutrient measurements taken between March 2013 and February 2014 by A. M. Messina (2018, personal communication) and analyzed in the lab as described in McCormick

(2017). Measurement uncertainty reported by McCormick (2017) for these samples was assessed by concurrently analyzing independent standards with known concentrations. Measurement error alone ranged from 7 % up to 30 %. Considering the limited number and large measurement error of the nitrogen observations, we focused nutrient calibration on producing the distribution of model solutions that bracketed as many of the observations as possible within the NSE 95% CI (Abbaspour et al., 2007). The final model calibration produced a solution distribution with a 95% CI that bracketed nine of the NH_4^+ measurements and fifteen of the NO_3^- measurements, which totaled to 60% of the calibration data (Fig 3.6b and 3.6c). Because of the high uncertainty in the nutrient calibration we interpreted these results as the full ranges of output values from all solutions that fell within the 95% CI distribution of the 1,000 best fitting model simulations (Table 3.2). In this way, large uncertainties in nutrient observations and in model parameterization were made explicit to avoid over interpretation of model results.

Sensitivity testing for all SWAT parameters was also performed with SWAT-CUP, and indicated the top three parameters to which the model was most sensitive for flow calibration were: (1) the runoff curve number, (2) the effective stream channel hydraulic conductivity, and (3) the threshold depth of water in the shallow aquifer required for return flow to occur. The top three most sensitive nutrient calibration parameters were: (1) the filtration capacity of stream edge, (2) the denitrification threshold soil water content, and (3) the in-stream rate constant for hydrolysis of organic N to NH_4^+. Lists of all calibration parameters used for flow and nutrient calibration are provided in Appendix C, Tables C3 and C4, respectively, and are ordered by the most to least sensitive parameter.

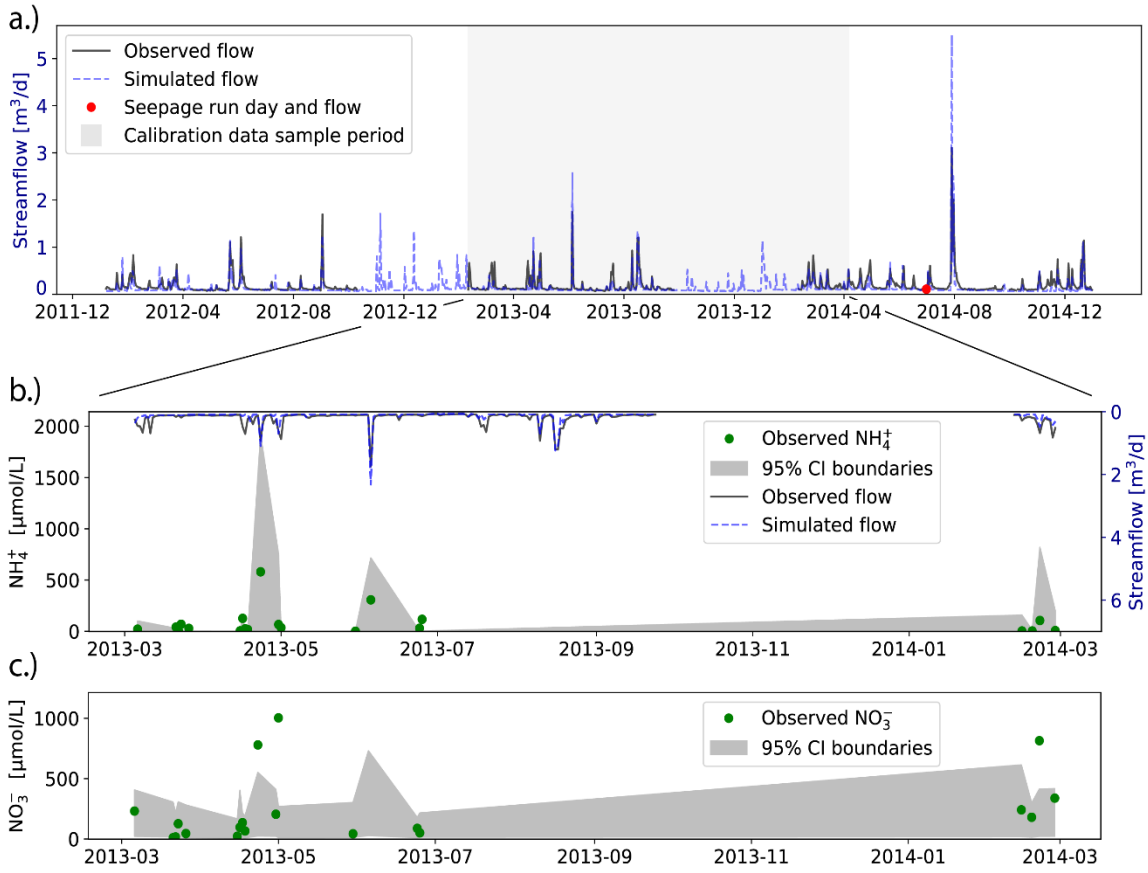

Figure 4.6: a) Daily streamflow hydrograph showing observed flow (from Messina, 2016) (black line) and SWAT modeled flow (blue dashed line). The date and flow value of our seepage run is indicated for comparative purposes (red dot). Shaded area corresponds to date range of nutrient calibration measurements as shown on lower panels. b) In–stream NH4+ concentrations taken by A.M. Messina, and used as calibration data for the nutrient flux portion of the SWAT model (green dots). Margins of the grey band represent the upper and lower bounds of the 95% confidence interval of simulated NH4+ concentrations from the distribution of solutions for which the model was calibrated. The model was able to bracket nine of the twenty NH4+ observations within the 95% CI. Streamflow is also shown on upper x-axis for comparison. c) In–stream NO3- concentrations taken by A.M. Messina and used as calibration data for the nutrient flux portion of the SWAT model. The model was able to bracket fifteen of the twenty NO3- observations within the 95% CI.

3.4.5.2 Simulated Water and Nutrient Fluxes

All coastally discharging water budget components, otherwise referred to as hydraulic pathways, were simulated in SWAT. These included baseflow, lateral flow, surface runoff, and SGD, which was interpreted to be equivalent to deep-aquifer recharge, as SGD is not an explicit SWAT model output variable. The SWAT model partitions precipitation inputs into evapotranspiration, surface runoff, lateral flow, and groundwater recharge, which is itself partitioned between deep aquifer recharge and baseflow. Using the assumption that the island's groundwater system is in a steady-state, the deep-aquifer recharge calculated by SWAT of 2,578

m^3/d was interpreted to represent the coastal SGD flux, as all water recharged to an island's deep aquifer must eventually discharge as SGD. High-level and basal-lens baseflow were also interpreted from SWAT results by applying our conceptual model, described in section 4.1. The conceptual model shows that stream baseflow originates from two distinctive aquifers, (1) the high-level aquifer and (2) the basal-lens aquifer. To approximate this scenario, we divided the SWAT-calculated baseflow into high-level baseflow and basal-lens baseflow by totaling baseflow from the sub-basins above and below the western margin of the alluvial unit, respectively. Based on this, the SWAT calculated baseflow of 3,203 m^3/d was partitioned into 2,075 m^3/d of high-level, or upper-watershed baseflow and 1,128 m^3/d of basal-lens, or lower watershed baseflow. Comparison between modeled and measured water balance components showed good agreement (Table 3.2). Although streamflow via surface runoff and lateral flow were not measured, the SWAT model provided estimates of these components at 5,888 m^3/d and 2,303 m^3/d, respectively, which sums to about 59% of the total annual stream flow.

Anthropogenic DIN sources used for N input in the SWAT model included piggeries, OSDS units, and agricultural inputs, which together accounted for 2,317 kg-N/yr of N loading to the watershed. The remainder of N inputs to the model were internally calculated in SWAT from natural cycling of organic materials, based on SWAT land-use databases. Because of the high-uncertainty resulting from less-than-ideal nutrient calibration, we here report SWAT nutrient loading results as ranges based on the upper and lower 95% CI bounds of the distribution of model solutions created during model calibration. Annual DIN export to the coast included simulated DIN in surface runoff, lateral flow, baseflow, and SGD. These flux rates are individually presented in Table 3.2, and when summed, ranged between 712 and 3,384 kg-DIN/yr. Ranges in individual components were large, but were to an order of magnitude, somewhat comparable to the measured baseflow and SGD-derived DIN fluxes, when simulated values were resampled to average daily fluxes (Fig. 4.7).

For validation purposes, direct comparison between SWAT-simulated and field-measured nutrient concentrations was examined for the date of July 1st, 2014, when the seepage run was conducted. The daily streamflow nutrient concentrations calculated by SWAT on the seepage run day were extracted from the best-fitting model run produced during calibration. Simulated nutrient concentrations at each of the points where samples were taken matched the spatial distribution and magnitude of measurements fairly well, with a simulated- to-observed mean relative error of 1.3 μmol/L (Fig. 4.7).

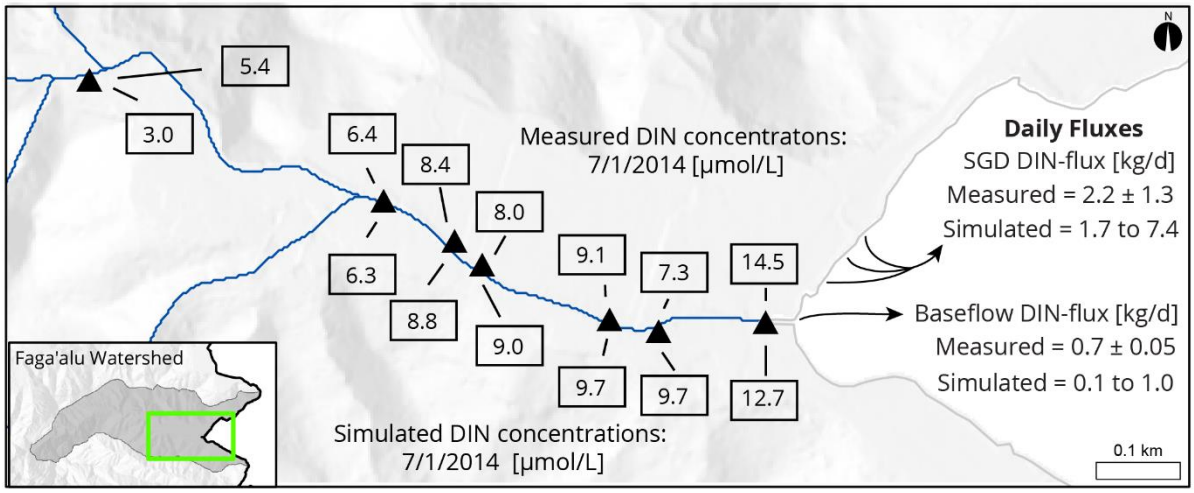

Figure 4.7: Comparison between measured and modeled nutrient results. Numbers in boxes show DIN concentrations (in µmol) at each sampling site specifically on the seepage run day (7/1/2014), with measured values north of the stream and simulated values to the south. Coastal DIN fluxes for SGD and for total baseflow (high-level plus basal-lens baseflows) are shown as daily rates (in kg of DIN per day). Note that average annual modeled DIN fluxes were scaled into daily fluxes for comparison to measured rates. Simulated fluxes do not necessarily represent flux rates on any specific day.

Table 3.2: Comparison of measured and modeled flux rates of fresh water and nutrients into Faga'alu Bay. Field-based nutrient fluxes are valid for the sampling period only, and are presented as daily values whereas SWAT modeled nutrient fluxes can be calculated as yearly or daily values, and are presented as both for comparison to measured fluxes. Modeled nutrient fluxes are reported as the upper and lower values of the 95% CI distribution of the 1,000 best fitting model simulations. Note that PO43- fluxes were measured but not modeled due to lack of calibration data.

Measured in field			
Hydrologic pathway	**Flow [m^3/d]**	**DIN load [kg-N/d]**	**PO_4^{3-} load [kg-P/d]**
High-level baseflow fraction	2,368 ± 238	0.25 + 0.02	0.22 + 0.02
Basal-lens baseflow fraction	1,157 ± 117	0.47 + 0.05	0.16 + 0.02
Coastal SGD fraction	2,587 ± 899	1.76 + 1.28	0.49 + 0.31

Modeled with SWAT				
Hydrologic pathway	**Flow [m^3/d]**	**DIN load [kg-N/yr]**	**Downsampled Daily DIN load for comparison [kg-N/d]**	
Upper watershed baseflow fraction	2,075	1 to 169	0.01 to 0.46	**Note: PO_4^{3-} was not modeled**
Lower watershed baseflow fraction	1,128	43 to 215	0.12 to 0.59	
Deep aquifer recharge (SGD) fraction	2,578	635 to 2,705	1.74 to 7.41	
Lateral flow fraction	2,303	19 to 507	0.05 to 1.39	
Surface runoff fraction	5,888	14 to 788	0.04 to 2.16	

3.4.5.3 Nutrient Loading Scenarios

We assessed the relative impact of each modeled non-point nutrient source within the watershed with four individual model scenarios, each with one, or all of the anthropogenic N sources removed. While these scenarios were not necessarily designed to reflect realistic future management actions, they were useful for estimating the relative impact each land-use practice has on coastal N loading. The N loading from each source was calculated by taking the difference of both the 95% CI lower and upper bounds, between the base-case and the scenario runs to produce 95% CI bracketed ranges of N-loading from each source. In general, scenarios suggested that of the three anthropogenic sources, OSDS units contribute the largest proportion of DIN, followed by piggeries, with agricultural loading as the least impactful. Interestingly, DIN transport from natural sources, which was assessed by removal of all anthropogenic sources, accounted for between 23 % and 99 % of the base-case DIN loads across the various hydrologic pathways (Table 3.3).

Table 3.3: Results of nutrient contribution scenarios. Base case values are presented as fluxes of nutrients in kg-DIN/yr and scenarios are presented as one minus the percent difference (% diff.) between each scenario and the base case. This indicates the fraction of the total DIN load contributed by each source to each hydrologic pathway.

Transport vector	Base case [Kg-DIN/yr.]	Agriculture contribution [% diff.]	OSDS contribution [% diff.]	Piggery contribution [% diff.]	Anthropogenic sources contribution [% diff.]	Natural sources contribution [% diff.]
Upper watershed baseflow	1 - 170	0.0% - 0.0%	0.0% - 0.0%	0.0% - 0.0%	0.0% - 0.0%	0.0% - 0.0%
Lower watershed baseflow	43 - 216	0.0% - 0.2%	99.0% - 44.7%	0.1% - 5.3%	99.1% - 50.0%	99.1% - 50.0%
SGD	636 – 2,705	0.0% - 0.4%	98.4% - 25.2%	0.2% - 8.9%	98.7% - 34.2%	98.7% - 34.2%
Lateral flow	20 - 507	0.0% - 0.1%	92.9% - 46.5%	3.1% - 1.5%	96.0% - 48.0%	96.0% - 48.0%
Surface Runoff	14 - 788	0.0% - 0.2%	6.9% - 5.0%	15.9% - 21.3%	22.8% - 26.3%	22.8% - 26.3%

3.5 Discussion

3.5.1 Implications for Natural Resources Management

Our results indicate SGD's contribution to coastal nutrient loading in Faga'alu is significant, particularly during baseflow conditions. We found nutrient loading from nearshore groundwater to be an order of magnitude higher than loads from high-level baseflow, and the SWAT model suggested DIN loading via groundwater may be significantly higher than loading from surface runoff, though this estimate excludes particulate-N. In American Samoa, coastal resource management efforts have primarily concentrated on surface water quality for regulatory activities (AS-EPA, 2016). Even on islands where SGD has been extensively studied, such as the Hawaiian Islands (e.g. Glenn et al., 2013; Dulai et al., 2016), little to no regulatory action has been focused on groundwater as a hydrologic pathway for pollution. Our field measurements and model results suggest that SGD and nearshore baseflow are important coastal nutrient delivery mechanisms in steep basaltic-island watersheds with perennial streams. In these settings, coastal management may be more successful if both ground and stream water quality are considered when developing sampling protocols and applying TMDL standards. Additionally, consideration of factors that affect the spatial and temporal distribution of nutrient discharge, such as variation in groundwater-surface water interaction and rainfall timing, will provide more robust and accurate assessment of human impacts on coastal ecosystems.

3.5.2 Conceptual Model Implications

In high-island settings, human development is typically concentrated on near-shore coastal plains that are often underlain by alluvium or marine sediments. If these sediments happen to be more permeable than the surrounding rock, as appears to be the case in Faga'alu, they may facilitate a more direct connection between anthropogenic contaminant sources and basal groundwater. In these settings, groundwater may play a larger role in coastal nutrient transport than surface water. However, the reverse may be true in settings where development is concentrated above less-permeable layers, which is the case in some parts of Oahu, Hawaii, where a locally low-permeability marine carbonate formation known as "caprock" protects the underlying aquifer from contaminants (Oki et al., 1998). Therefore, in basaltic-island settings, the partitioning of nutrients from non-point sources into different hydrologic pathways is likely to be highly dependent on the relative permeabilities of different nearshore geologic layers. This farther underscores the importance of developing a reasonably accurate conceptualization of local hydrogeologic systems when designing sampling schemes and assessing nutrient fluxes on a ridge-to-reef scale.

The high-resolution, locality specific understanding of groundwater-surface water interaction we developed for Faga'alu helped with construction and interpretation of the SWAT model. Discharge or loss between groundwater and a stream is generally controlled by water table elevation, which makes this parameter very important for predicting the distribution of baseflow in a watershed. However, the SWAT model uses a simplified linear reservoir model to control loss or gain from groundwater and does not consider water table elevations for baseflow partitioning. This gap is commonly filled by coupling surface water models with groundwater models (e.g. Kim et al., 2008; Guzman et al., 2015). However, subsurface models rely on calibrated parameterization of stream conductance and hydraulic conductivity, and in settings such as Faga'alu, the variable and steep terrain (Kampf and Burges, 2007) as well as a lack of groundwater elevation data (apart from one single well in the valley) imparts an unacceptable amount of uncertainty to groundwater modeling attempts. To cope with this challenge, we used a reasonable conceptual hydrogeologic model to determine where the water table was generally below the stream elevation (losing reach below the quarry) and where it was at or above the stream (gaining reach above the quarry). This provided the justification to allow for partitioning fluxes from high-level and basal-lens baseflow, likely within the same amount of certainty as would have been achieved through a more time-consuming and costly groundwater modeling process.

3.5.3 Nitrogen Source Tracing

While extensive source dependent nutrient tracing efforts were not performed in this study, reasonable correlation between elevated DIN concentrations and $\delta^{15}N$ isotopes in baseflow and coastal surface water (r^2 of 0.93 and 0.45, respectively) helped to validate the

transport history of nutrients from source to sink. High values of $\delta^{15}N$ that are correlated with high DIN values suggests the majority of the DIN found in samples originates from a high $\delta^{15}N$ source, such as wastewater or manure, as opposed to synthetic agricultural fertilizers, which typically have $\delta^{15}N$ values near 0 ‰ (Kendall and Aravena, 2000). Finding this result in Faga'alu was not surprising, considering that most agricultural operations in the valley are small and focused on traditional Samoan crops that require few to no chemical inputs. However, a more pertinent need in American Samoa is to prioritize management of either piggeries or OSDS-sourced wastewater, because limited management resources could be more effectively spent if the relative impact from each source was better constrained (Carpenter et al., 2002; Shuler et al., 2017). Unfortunately, the overlap of $\delta^{15}N$ values from animal manure and wastewater (Böhlke, 2003) does not allow DIN from these sources to be reliably partitioned with this method. Another complicating factor with isotopic N source tracing is mixing of nutrients from different sources, which would alter the final isotopic composition found in samples. More specific source-dependent tracers, like microbial source tracing (Scott et al., 2002; Kirs et al., 2011) or wastewater specific compounds (Petrie et al., 2015; Krall et al., 2018) would be useful for separating and prioritizing the impacts between wastewater and pigs in Samoa.

3.5.4 SWAT Model Applicability

The SWAT model was useful for providing insights into nutrient loading from processes and time periods that were not assessed during the field investigation. Due to the logistics of working in a remote area, our fieldwork was limited to a single week, thereby limiting the representativeness of measured nutrient fluxes to this time-period and season. For management priorities however, annual nutrient fluxes are more useful for assessing longer-term management questions. Compounding this is the fact that streams on small islands are generally steep and flashy, making it time-consuming to sample runoff events at a resolution that effectively characterizes annual nutrient fluxes (De Carlo et al., 2007). The SWAT model filled this gap in our study by providing daily resolution flows and loading rates that could be totalized to estimate annual discharge and DIN loading from each hydrologic pathway. This is highly beneficial for understanding processes that are prohibitively difficult or costly to observe, such as assessment of lateral flow or surface runoff, and allows a more comprehensive understanding of water and nutrient transport dynamics in difficult-to-study or remote watersheds.

Despite high uncertainties associated with simulated nutrient flux results, the model nonetheless proved useful for partitioning the impact from each anthropogenic non-point source through a scenario-based approach of modifying land-use inputs. When the effects of individual non-point sources were each removed from the input, results indicated a significant proportion of DIN in subsurface hydrologic pathways, including SGD, lateral flow, and baseflow, originating from OSDS sources. The proportion of OSDS sourced DIN in all

pathways, except for surface runoff, ranged from 25 % to 99 % of the base-case DIN discharge. On the other hand, OSDS loading appeared to contribute very little to DIN loads in surface runoff, less than 7 % (Table 3.3). Of the three modeled anthropogenic sources, piggeries appeared to contribute the most DIN to surface runoff, between 16 % and 21 %. The contribution of piggery DIN to groundwater was lower, less than 9 % of the total DIN in SGD or baseflow. This pattern is reasonable since OSDS leachate and manure are discharged into the environment in different ways. Subsurface OSDS units leach N directly below the soil, whereas pig manure is typically released directly on the land surface; and in American Samoa, manure is sometimes washed directly into streams, although this practice is currently illegal. This indicates that management focused on reducing OSDS impact is likely to primarily affect groundwater nitrogen loads, but if surface water quality is deemed to be more important, then management of piggeries may be a more effective strategy. As expected, removal of all agricultural sources did very little to affect modeled DIN fluxes considering the low magnitude of agricultural loading inputs.

While human land-use activities are often considered to be the primary cause of nutrient-based water quality impairment, nutrient inputs from natural plant and animal sources should not be ignored. For example, on Tutuila, Nimbus Environmental Services (2010) found that coastal water samples frequently exceeded local and federal water quality standards for PO_4^{3-} concentrations, even in lightly impacted areas. They concluded that geologic sources on Tutuila may produce naturally high levels of PO_4^{3-} in source waters. This has also been observed in the Hawaiian Islands (Vitousek et al. 2003). While an ideal approach to assess natural nutrient loads would be to duplicate study methodologies in pristine control watersheds, it is often difficult to even find pristine watersheds on islands where land is scarce, and if available, these areas often lack road access, which significantly complicates field logistics. Since this was not possible in our study, we estimated naturally-sourced DIN loading using a SWAT model scenario with all anthropogenic nutrient sources removed. Results suggested that coastal DIN loading from natural sources is somewhere between 20 and 2,734 kg-DIN/yr. When compared to the base case scenario, these results suggest that natural sources contribute between 74 % and 77% of DIN in surface runoff, 4 % to 52 % of DIN in lateral flow, 2 % to 70 % of DIN in baseflow and 1 % to 65 % of DIN in SGD. While these ranges are large, this result does suggest that natural nutrient sources are important to consider in this setting; however anthropogenic sources are still likely to be the main cause of elevated nutrient concentrations seen in Faga'alu Watershed. While complete removal of any of the watershed's non-point sources is not very realistic, the ability to run these different scenarios showed the relative impact of each source and also helped to validate the idea that management focused on different sources may benefit from adopting different sampling and assessment strategies.

3.5.5 Assumptions and Limitations of the SWAT Model

1. The SWAT model uses a simplified linear reservoir model for the representation of the groundwater system, which applies a single parameter (RCHRG_DP) for total

groundwater recharge partitioning to the deep aquifer (interpreted here as SGD). Hence, SWAT's SGD results are somewhat sensitive to this parameter (Appendix C, Table C3). Additionally, this interpretation hinges on the assumption that watershed boundaries also represent aquifer divides. Nonetheless, when the RCHRG_DP parameter was calibrated to match measured SGD, the model was able to match streamflow observations well, suggesting that SWAT's parameterization was reasonable.

2. The daily N loading rates from anthropogenic sources (OSDS, piggeries, and fertilizers,) were assumed to be constant due to a lack of information about application timing. However, probably only OSDS loading is actually constant. Agricultural applications, and the number of pigs in a piggery at any given time likely fluctuates cyclically. Because agriculture is practiced year-round in American Samoa, it is difficult to predict when applications occur.

3. The SWAT model was calibrated with streamflow data from two stations, (*black diamonds* in Fig. 3.2) and therefore different parameter values were assigned for the upper watershed above the quarry, and for the lower watershed below. This was justified geologically, considering that the quarry location coincides with the contact between basalts and alluvium. However, in reality, the local geology is probably heterogeneous, particularly within the basalt unit itself. Thus the bi-modal parameterization of the model area is likely to be somewhat of an oversimplification.

4. Very limited information exists regarding septic system design in American Samoa. It is thought that many of the island's residents rely on cesspools (Falkland et al., 2002). However, exact numbers and specificities about system design remain unknown. Therefore, in SWAT, OSDS units were simulated with default parameters and an assumption that all systems were of a failing septic system type (TCE, 2005).

5. The lack of long term, multi-year measured in-stream nutrient data necessitated a heuristic approach where only order-of-magnitude scale nutrient fluxes could be confidently calculated and reported.

3.6 Conclusions

By combining a terrestrial and coastal hydrologic field investigation with model-based watershed characterization we were able to reveal the impact of different nutrient sources and hydrologic pathways in a small American Samoan watershed. This methodological framework demonstrates how snapshot scale observations and transient watershed modeling can be integrated to develop a fairly comprehensive understanding of water and nutrient dynamics in steep watersheds on tropical-basaltic islands. In Faga'alu Watershed, during low-flow conditions, our measurements suggested SGD and nearshore basal-lens baseflow contribute nearly all of the terrigenous DIN to the coastline with high level-baseflow contributing very little. Groundwater discharge was also found to be significant in coastal loading of dissolved PO_4^{3-}. Seepage run measurements indicated groundwater discharge to the stream occurs as two geochemically distinct fractions, (1) high-level baseflow and (2) basal-lens baseflow that discharges near the stream estuary. At baseflow conditions, high-level streamflow was seen to contribute about two-thirds of the stream's water, but nearshore basal-lens baseflow contributed the majority of the stream's nutrient load. This understanding of groundwater – surface water interaction proved useful for the conceptual foundation for developing the watershed model and for interpreting model results.

The SWAT model matched fluxes from measured water budget components well, within 2 %, 13 %, and 0.3 % RPD for basal-lens baseflow, high-level baseflow, and SGD, respectively. Despite limitations in nutrient calibration, SWAT was also able to provide order-of-magnitude estimates of nutrient fluxes over annual scales and from components such as surface runoff and lateral flow, which could not be measured during fieldwork. Though uncertainties were large, the model suggested that storm and lateral flow together deliver between 5 % and 31 % of the total annual DIN load. This leaves groundwater sources as the most impactful nutrient transport pathways, with SGD-derived DIN loading making up between 65 % to 92 % of the total annual DIN loading to the coast, and the remainder being delivered by baseflow. This suggests that both SGD and surface water are important coastal nutrient loading pathways and both should be considered when developing nutrient sampling and management plans. Although sampling surface runoff, baseflow, and groundwater nutrients would require a significant deviation from current water quality management practice and assessment in American Samoa, if watershed models can be developed to account for these processes, they can be a useful and money-saving tool in the land-manager's toolbox.

References: Chapter 3

Abbaspour, K.C., 2014. SWAT-CUP 2012: SWAT Calibration and Uncertainty Programs - A User Manual. Sci. Technol. https://swat.tamu.edu/media/114860/usermanual_swatcup.pdf (accessed 2019-03-13).

Alexander, R.B., Elliott, A.H., Shankar, U., McBride, G.B., 2002. Estimating the sources and transport of nutrients in the Waikato River Basin, New Zealand. Water Resour. Res. 38, 4-1-4–23. https://doi.org/10.1029/2001wr000878

Amato, D.W., Bishop, J.M., Glenn, C.R., Dulai, H., Smith, C.M., 2016. Impact of submarine groundwater discharge on marine water quality and reef biota of Maui. PLoS One 11, e0165825. https://doi.org/10.1371/journal.pone.0165825

AS-EPA - American Samoa Environmental Protection Agency, 2010. Territory of American Samoa Integrated Water Quality Monitoring and Assessment 2010. https://www.epa.as.gov/sites/default/files/documents/surface/americansamoa2010integratedwaterqualityreport031910.pdf (accessed 2019-03-13).

Andreani, M., Galanter, M., Casciotti, K.L., Böhlke, J.K., Sigman, D.M., Barford, C., 2002. A Bacterial Method for the Nitrogen Isotopic Analysis of Nitrate in Seawater and Freshwater. Anal. Chem. 73, 4145–4153. https://doi.org/10.1021/ac010088e

Armstrong, F.A.J., Stearns, C.R., Strickland, J.D.H., 1967. The measurement of upwelling and subsequent biological process by means of the Technicon Autoanalyzer® and associated equipment, in: Deep-Sea Research and Oceanographic Abstracts. pp. 381–389. https://doi.org/10.1016/0011-7471(67)90082-4

Arnold, J.G., Srinivasan, R., Muttiah, R.S., Williams, J.R., 1998. Large area hydrologic modeling and assessment part I: Model development. J. Am. Water Resour. Assoc. 34, 73–89. https://doi.org/10.1111/j.1752-1688.1998.tb05961.x

ASCC – American Samoa Community College, 2018. Malaeimi weather station data. [Dataset]. https://www.wunderground.com/personal-weather-station/dashboard?ID=IWESTERN499 (accessed 2018-04-30).

AS-DOC – American Samoa Department of Commerce, 2013. 2013 Statistical Yearbook for American Samoa. http://doc.as.gov/wp-content/uploads/2011/06/2013-Statistical-Yearbook-Final-Draft.pdf (accessed 2019-03-13).

AS-EPA - American Samoa Environmental Protection Agency,, 2013. American Samoa Water Quality Standards 2013 Revision Administrative Rule No . 001-2013. https://www.epa.gov/sites/production/files/2014-12/documents/aswqs.pdf (accessed 2019-03-13).

AS-EPA - American Samoa Environmental Protection Agency, 2013. American Samoa Watershed Management and Protection Program FY08 Annual Report.

Avery, E., Bibby, R., Visser, A., Esser, B., Moran, J., 2018. Quantification of groundwater discharge in a subalpine stream using radon-222. Water (Switzerland) 10, 100. https://doi.org/10.3390/w10020100

Babinec, J., Kennedy, J., Williamson, M., Kamenik, J., Waters, C.A., Jolly, J., Dulai, H., 2015. Autonomous long-term gamma-spectrometric monitoring of submarine groundwater discharge trends in Hawaii. J. Radioanal. Nucl. Chem. 307, 1865–1870. https://doi.org/10.1007/s10967-015-4580-9

Bahr, K.D., Jokiel, P.L., Toonen, R.J., 2015. The unnatural history of Kāne'ohe Bay: coral reef resilience in the face of centuries of anthropogenic impacts. PeerJ 3, e950. https://doi.org/10.7717/peerj.950

Barden, R., Kasprzyk-Hordern, B., Petrie, B., 2015. A review on emerging contaminants in wastewaters and the environment: Current knowledge, understudied areas and recommendations for future monitoring. Water Res. 72, 3–27.

Böhlke, J.-K., 2003. Sources, transport, and reaction of nitrate., Residence times and nitrate transport in ground water discharging to streams in the Chesapeake Bay Watershed. Water-Resources Investiagations.

Buchanan, T.J., Somers, W.P., 1976. Discharge measurements at gaging stations, Techniques of water-resources investigations of the United States Geological Survey - Book 3 - Applications of Hydarulics.

Burnett, W.C., Dulaiova, H., 2003. Estimating the dynamics of groundwater input into the coastal zone via continuous radon-222 measurements. J. Environ. Radioact. 69, 21–35. https://doi.org/10.1016/S0265-931X(03)00084-5

Carpenter, C., Stubbs, J., Overmars, M., 2003. Proceedings of the Pacific Regional Consultation On Water in Small Island Countries.

Carpenter, C., Stubbs, J., Overmars, M., 2003. Proceedings of the Pacific Regional Consultation On Water in Small Island Countries.

Chadwick, O., Porder, S., Luers, A., Monastra, V., Kettley, L., Matson, P., Derry, L., Mecking, E., Allison, S., Vitousek, P., 2004. Erosion and the Rejuvenation of Weathering-derived Nutrient Supply in an Old Tropical Landscape. Ecosystems 6, 762–772. https://doi.org/10.1007/s10021-003-0199-8

Charette, M. a, Moore, W.S., Burnett, W.C., 2007. CHAPTER-5 Uranium-and Thorium- Series Nuclides as Tracers of Submarine Groundwater Discharge CHAPTER-5 Uranium-and

Thorium-Series Nuclides as Tracers of Submarine Groundwater Discharge. Uranium 13, 234–289.

Cole, M.L., Kroeger, K.D., McClelland, J.W., Valiela, I., 2006. Effects of Watershed Land use on Nitrogen Concentrations and delta15 Nitrogen in Groundwater \h [electronic resource]. Biogeochemistry 77, 199–215.

D. K. Borah, M. Bera, 2013. Watershed-Scale Hydrologic and Nonpoint-Source Pollution Models: Review of Applications. Trans. ASAE 47, 789–803. https://doi.org/10.13031/2013.16110

Davis, D., 1963. Groundwater reconnaissance of American Samoa. U.S. Geological Survey Report No. 1608-C. US Government Printing Office.

DiDonato, G.T., 2005. Nitrogen and phosphorus concentrations in tropical Pacific insular streams: historical data from Tutuila, American Samoa. Micronesica-Agana- 37, 235.

Downer, C.W., Ogden, F.L., 2006. Gridded Surface Subsurface Hydrologic Analysis (GSSHA) User's Manual, Version 1.43 for Watershed Modeling System 6.1, US Army Corps of Engineers, Engineer Research and Development Center.

Dulaiova, H., Burnett, W.C., Wattayakorn, G., Sojisuporn, P., 2006. Are groundwater inputs into river-dominated areas important? The Chao Phraya River - Gulf of Thailand. Limnol. Oceanogr. 51, 2232–2247. https://doi.org/10.4319/lo.2006.51.5.2232

Dulaiova, H., Camilli, R., Henderson, P.B., Charette, M.A., 2010. Coupled radon, methane and nitrate sensors for large-scale assessment of groundwater discharge and non-point source pollution to coastal waters. J. Environ. Radioact. 101, 553–563. https://doi.org/10.1016/j.jenvrad.2009.12.004

Fröllje, H., Fitzsimmons, J.N., Dulai, H., Schnetger, B., Brumsack, H.-J., Pahnke, K., 2016. Hawaiian imprint on dissolved Nd and Ra isotopes and rare earth elements in the central North Pacific: Local survey and seasonal variability. Geochim. Cosmochim. Acta 189, 110–131. https://doi.org/10.1016/j.gca.2016.06.001

Gardner, L.R., Wilson, A.M., 2006. Comparison of four numerical models for simulating seepage from salt marsh sediments. Estuar. Coast. Shelf Sci. 69, 427–437. https://doi.org/10.1016/j.ecss.2006.05.009

P. W. Gassman, M. R. Reyes, C. H. Green, J. G. Arnold, 2007. The Soil and Water Assessment Tool: Historical Development, Applications, and Future Research Directions. Trans. ASABE 50, 1211–1250. https://doi.org/10.13031/2013.23637

Gassman, P.W., Sadeghi, A.M., Srinivasan, R., 2014. Applications of the SWAT Model Special Section: Overview and Insights. J. Environ. Qual. 43, 1. https://doi.org/10.2134/jeq2013.11.0466

Garrison, V., Kroeger, K., Fenner, D., Craig, P., 2007. Identifying nutrient sources to three lagoons at Ofu and Olosega, American Samoa using δ15N of benthic macroalgae. Mar. Pollut. Bull. 54, 1830–1838. https://doi.org/10.1016/j.marpolbul.2007.08.016

Gillespie, P., Kirs, M., Cornelisen, C., Fidler, A., Harwood, V., Blackwood, A., Fyfe, W., 2011. Source tracking faecal contamination in an urbanised and a rural waterway in the Nelson-Tasman region, New Zealand. New Zeal. J. Mar. Freshw. Res. 45, 43–58. https://doi.org/10.1080/00288330.2010.535494

Gleeson, J., Santos, I.R., Maher, D.T., Golsby-Smith, L., 2013. Groundwater-surface water exchange in a mangrove tidal creek: Evidence from natural geochemical tracers and implications for nutrient budgets. Mar. Chem. 156, 27–37. https://doi.org/10.1016/j.marchem.2013.02.001

Gleeson, T., Manning, A.H., Popp, A., Zane, M., Clark, J.F., 2018. The suitability of using dissolved gases to determine groundwater discharge to high gradient streams. J. Hydrol. 557, 561–572. https://doi.org/10.1016/j.jhydrol.2017.12.022

Glenn, C.R., Whittier, R.B., Dailer, M.L., Dulaiova, H., El-kadi, A.I., Fackrell, J., Sevadjian, J., 2013. Lahaina Groundwater Tracer Study —Lahaina, Maui, Hawaii. Final Interim Report prepared from the State of Hawaii DOH, the U.S. EPA, and the U.S. Army Engineer Research and Development Center https://scholarspace.manoa.hawaii.edu/handle/10125/50768 (accessed 2019-03-13).

Grasshoff, K., Ehrhardt, M., Kremling, K., 1999. Methods of Seawater Analysis. Second, Revised and Extended Edition, 3rd ed. John Wiley & Sons.

Guzman, J.A., Moriasi, D.N., Gowda, P.H., Steiner, J.L., Starks, P.J., Arnold, J.G., Srinivasan, R., 2015. Environmental Modelling & Software A model integration framework for linking SWAT and MODFLOW. Environ. Model. Softw. 73, 103–116. https://doi.org/10.1016/j.envsoft.2015.08.011

Houk, P., Didonato, G., Iguel, J., & Van Woesik, R., 2005. Assessing the effects of non-point source pollution on American Samoa's coral reef communities. Environ. Monit. Assess. 107, 11–27.

Houk, P., Benavente, D., Johnson, S., 2013. Watershed-based coral reef monitoring across Tutuila, American Samoa - Summary of decadal trends and 2013 assessment.

Hunt, C.D., 2006. Ground-Water Nutrient Flux to Coastal Waters and Numerical Simulation of Wastewater Injection at Kihei , Maui , Hawaii. USGS Open Report 2006, 5283. https://pubs.usgs.gov/sir/2006/5283/sir2006-5283.pdf (accessed 2019-03-13).

Hunt, Charles D., J., Rosa, S.N., 2009. A Multitracer Approach to Detecting Wastewater Plumes from Municipal Injection Wells in Nearshore Marine Waters at Kihei and Lahaina, Maui, Hawaii (USGS Scientific Investigations Report 2009-5253) 166.

Izuka, S.K., Perreault, J.A., Presley, T.K., 2007. Areas contributing recharge to wells in the Tafuna-Leone Plain, Tutuila, American Samoa: U.S. Geological Survey Scientific Investigations Report 2007-5167.

Johannes, R.E., Hearn, C.J., 1985. The effect of submarine groundwater discharge on nutrient and salinity regimes in a coastal lagoon off Perth, Western Australia. Estuar. Coast. Shelf Sci. 21, 789–800. https://doi.org/10.1016/0272-7714(85)90073-3

Kampf, S.K., Burges, S.J., 2007. A framework for classifying and comparing distributed hillslope and catchment hydrologic models. Water Resour. Res. 43. https://doi.org/10.1029/2006WR005370

Kelly, J.L., Glenn, C., 2012. Identification and quantification of submarine groundwater discharge in the Hawaiian Islands. Dep. Geol. Geophys. [Honolulu]:[University of Hawaii at Manoa],[August 2012].

Kendall, C., 2012. Tracing Nitrogen Sources and Cycling in Catchments, in: Isotope Tracers in Catchment Hydrology. Elsevier, pp. 519–576. https://doi.org/10.1016/b978-0-444-81546-0.50023-9

Kendall, C., Aravena, R., 2011. Nitrate Isotopes in Groundwater Systems, in: Environmental Tracers in Subsurface Hydrology. Springer, pp. 261–297. https://doi.org/10.1007/978-1-4615-4557-6_9

Kim, N. W., Chung, I. M., Won, Y. S., & Arnold, J.G., 2008. Development and application of the integrated SWAT-MODFLOW model. Journal. of. Hydrol. 356, 1–16.

Krall, A.L., Elliott, S.M., Erickson, M.L., Adams, B.A., 2018. Detecting sulfamethoxazole and carbamazepine in groundwater: Is ELISA a reliable screening tool? Environ. Pollut. 234, 420–428. https://doi.org/10.1016/j.envpol.2017.11.065

Lindau, Delaune, Patr, 1989. Assessment of stable n isotopes in fingerprinting surface water n source. Water. Air. Soil Pollut. 48, 489–496.

Makings, U., Santos, I.R., Maher, D.T., Golsby-Smith, L., Eyre, B.D., 2014. Importance of budgets for estimating the input of groundwater-derived nutrients to an eutrophic tidal river and estuary. Estuar. Coast. Shelf Sci. 143, 65–76. https://doi.org/10.1016/j.ecss.2014.02.003

Messina, A.M., Biggs, T.W., 2016. Contributions of human activities to suspended sediment yield during storm events from a small, steep, tropical watershed. J. Hydrol. 538, 726–742. https://doi.org/10.1016/j.jhydrol.2016.03.053

McCormick, G.R., 2017. Water Quality and Sources of Nutrient Loads in Watersheds of American Samoa. Masters thesis, Dept. of Geography, San Diego State University. https://search.proquest.com/openview/a236c90fb2b272eab29080873da04169/1?pq-origsite=gscholar&cbl=18750&diss=y (accessed 2019-03-13).

Messina, A.T., 2013. Terrestrial Sediment and Nutrient Fluxes to the Faga'alu Reefs in American Samoa, in: AGU Fall Meeting Abstracts. p. 08.

Messina, A.T., 2016. Terrigenous Sediment Dynamics in a Small, Tropical Fringing-Reef Embayment, American Samoa. Doctoral dissertation Dept. of Geography, University of California, Santa Barbara. https://www.alexandria.ucsb.edu/lib/ark:/48907/f3sj1kpt (accessed 2019-03-13).

Michael, H.A., 2005. Seasonal dynamics in costal aquifers: investigation of submarine groundwater discharge through field measurements and numerical models. Environ. Eng. Massachusetts Institute of Technology.

Moosdorf, N., Stieglitz, T., Waska, H., Dürr, H., Hartmann, J., 2015. Submarine groundwater discharge from tropical islands: a review. Grundwasser 20, 53–67. https://doi.org/10.1007/s00767-014-0275-3

Morrissey, A., Nolan, K., Rock, L., Fenech, C., Tobin, J., 2012. The potential for a suite of isotope and chemical markers to differentiate sources of nitrate contamination: A review. Water Res. 46, 2023–2041. https://doi.org/10.1016/j.watres.2012.01.044

Nakamura, S., 1984. Soil Survey of American Samoa. USDA Soil Conservation Service, Washington, DC. 95 pp

NGDC, 2013. American Samoa 1/3 Arc-second MWH Coastal Digital Elevation Model [dataset]. https://catalog.data.gov/dataset/pago-pago-american-samoa-coastal-digital-elevation-model34341 (accessed 2015-12-10).

Nimbus Environmental Services, 2012. US EPA National Coastal Assessment 2010, American Samoa Reef Flats, 2012.

NOAA, 2013. Faga'alu Village Watershed Management and Conservation Plan. ftp://ftp.library.noaa.gov/noaa_documents.lib/CoRIS/Faga'alu_Village_Watershed.pdf

Oberdorfer, J.A., 2003. Hydrogeologic modeling of submarine groundwater discharge: Comparison to other quantitative methods. Biogeochemistry 66, 159–169. https://doi.org/10.1023/B:BIOG.0000006096.94630.54

Oki, D.S., Souza, W.R., Bolke, E.L., Bauer, G.R., 1998. Numerical analysis of the hydrogeologic controls in a layered coastal aquifer system, Oahu, Hawaii, USA. Hydrogeol. J. 6, 243–263. https://doi.org/10.1007/s100400050149

Paul, S., Cashman, M.A., Szura, K., Pradhanang, S.M., 2017. Assessment of nitrogen inputs into hunt river by onsite wastewater treatment systems via SWAT simulation. Water (Switzerland) 9, 610. https://doi.org/10.3390/w9080610

Peterson, R.N., Santos, I.R., Burnett, W.C., 2010. Estuarine , Coastal and Shelf Science Evaluating groundwater discharge to tidal rivers based on a Rn-222 time-series approach. Estuar. Coast. Shelf Sci. 86, 165–178. https://doi.org/10.1016/j.ecss.2009.10.022

Polidoro, B.A., Comeros-Raynal, M.T., Cahill, T., Clement, C., 2017. Land-based sources of marine pollution: Pesticides, PAHs and phthalates in coastal stream water, and heavy metals in coastal stream sediments in American Samoa. Mar. Pollut. Bull. 116, 501–507. https://doi.org/10.1016/j.marpolbul.2016.12.058

Rengarajan, R., Sarma, V.V.S.S., 2015. Submarine groundwater discharge and nutrient addition to the coastal zone of the Godavari estuary. Mar. Chem. 172, 57–69. https://doi.org/10.1016/j.marchem.2015.03.008

Rogers, K.M., Nicolini, E., Gauthier, V., 2012. Identifying source and formation altitudes of nitrates in drinking water from Réunion Island, France, using a multi-isotopic approach. J. Contam. Hydrol. 138–139, 93–103. https://doi.org/10.1016/j.jconhyd.2012.07.002

Rosenberry, D.O., LaBaugh, J.W., 2008. Field Techniques for Estimating Water Fluxes Between Surface Water and Ground Water Techniques and Methods 4 – D2, U. S. Geological Survey.

S. Pradhan, J. Jeong, K. Flynn, R. Srinivasan, J. G. Arnold, C. Santhi, 2013. Development of Algorithms for Modeling Onsite Wastewater Systems within SWAT. Trans. ASABE 54, 1693–1704. https://doi.org/10.13031/2013.39849

Sadat-Noori, M., Santos, I.R., Sanders, C.J., Sanders, L.M., Maher, D.T., 2015. Groundwater discharge into an estuary using spatially distributed radon time series and radium isotopes. J. Hydrol. 528, 703–719. https://doi.org/10.1016/j.jhydrol.2015.06.056

Saito, M., Onodera, S., Ohta, T., Shimizu, Y., Zhu, A., Jin, G., Chen, J., 2018. Evaluation of the spatial distribution of submarine groundwater discharge in a small island scale using the 222Rn tracer method and comparative modeling, in: editor, T. (Ed.), Marine Chemistry. Honolulu, HI. https://doi.org/10.1016/j.marchem.2018.12.003

Schwarz, G.E., Hoos, A.B., Alexander, R.B., Smith, R.A., 2006. The SPARROW Surface Water-Quality Model: Theory, Application and User Documentation: U.S. Geological Survey Techniques and Methods Book 6, Section B, Chapter 3. US Geol. Surv. Tech. methods report, B. 6, 248.

Scott, T.M., Rose, J.B., Jenkins, T.M., Farrah, S.R., 2002. Microbial Source Tracking : Current Methodology and Future Directions †. Appl. Environ. Microbiol. 68, 5796–5803. https://doi.org/10.1128/AEM.68.12.5796

Shuler, C.K., El-Kadi, A.I., Dulai, H., Glenn, C.R., Fackrell, J., 2017. Source partitioning of anthropogenic groundwater nitrogen in a mixed-use landscape, Tutuila, American Samoa . Hydrogeol. J. 25, 2419–2434. https://doi.org/10.1007/s10040-017-1617-x

Stearns, H.T., 2015. Geology of the Samoan Islands. Geol. Soc. Am. Bull. 55, 1279–1332. https://doi.org/10.1130/gsab-55-1279

Storlazzi, C., Messina, A., Cheriton, O., Biggs, T., 2014. Eulerian and Lagrangian Measurements of Water Flow and Residence Time in a Fringing Coral Reef Embayment, in: AGU Fall Meeting Abstracts.

Takasaki, K.J., Mink, J.F., 1985. Evaluation of major dike-impounded ground-water reservoirs, Island of Oahu, U.S. Geological Survey Water Supply Paper 2217. US Government Printing Office Washington, DC.

TCE, 2005. OWTS 201: Overview of Advanced Wastewater Treatment Systems, Manual published by the Texas A&M University System. https://ossf.tamu.edu/educational-materials-2/ (accessed 2015-12-10).

The World Bank, 2014. Fertilizer consumption (kilograms per hectare of arable land). World Dev. Indic. http://data.worldbank.org/indicator/AG.CON.FERT.ZS?page=2 (accessed 2017 -02 -17).

Thomas, F., Ruttenberg, K., Dulai, H., Kleven, A., Briggs, R., 2016. Evaluation of Submarine Groundwater Discharge as a Coastal Nutrient Source and Its Role in Coastal Groundwater Quality and Quantity, in: Fares, A. (Ed.), Emerging Issues in Groundwater Resources. Springer, Prairie View, TX, pp. 187–221. https://doi.org/10.1007/978-3-319-32008-3_8

Thomas, F., Ruttenberg, K., Dulai, H., Kleven, A., Briggs, R., 2016. Evaluation of Submarine Groundwater Discharge as a Coastal Nutrient Source and Its Role in Coastal Groundwater Quality and Quantity, in: Emerging Issues in Groundwater Resources. Springer, pp. 187–221. https://doi.org/10.1007/978-3-319-32008-3_8

Vetter, O., Vargas-Angel, B., 2014. CRCP Project # 417 : Inter-Disciplinary Study of Flow Dynamics and Sedimentation Effects on Coral Colonies in Faga'alu Bay, American Samoa : Oceanographic Investigation Summary. Pago Pago.

Weinstein, Y., Masqué, P., Feldman, M., Rodellas, V., Garcia-Orellana, J., 2015. Submarine groundwater discharge as a major source of nutrients to the Mediterranean Sea. Proc. Natl. Acad. Sci. 112, 3926–3930. https://doi.org/10.1073/pnas.1419049112

Whitall, D.R., Rice, S.H., 2015. Pollution in surface sediments in Faga'alu Bay, Tutuila, American Samoa. NOAA Technical Memorandum NOS NCCOS 201. Silver Spring, MD. 54 pp. https://coastalscience.noaa.gov/data_reports/pollution-in-surface-sediments-in-fagaalu-bay-tutuila-american-samoa/t (accessed 2019-03-13).

Wiegner, T.N., Mokiao-Lee, A.U., Johnson, E.E., 2016. Identifying nitrogen sources to thermal tide pools in Kapoho, Hawai'i, U.S.A, using a multi-stable isotope approach. Mar. Pollut. Bull. 103, 63–71. https://doi.org/10.1016/j.marpolbul.2015.12.046

Wong, W.W., Grace, M.R., Cartwright, I., Cook, P.L.M., 2014. Sources and fate of nitrate in a groundwater-fed estuary elucidated using stable isotope ratios of nitrogen and oxygen. Limnol. Oceanogr. 59, 1493–1509. https://doi.org/10.4319/lo.2014.59.5.1493

Yang, J., Maximov, I., Srinivasan, R., Zobrist, J., Mieleitner, J., Abbaspour, K.C., Siber, R., Bogner, K., 2006. Modelling hydrology and water quality in the pre-alpine/alpine Thur watershed using SWAT. J. Hydrol. 333, 413–430. https://doi.org/10.1016/j.jhydrol.2006.09.014

Young, C.W., Hoover, D.J., DeCarlo, E.H., MacKenzie, F.T., McManus, M.A., 2005. Impact of storm runoff from subtropical watersheds on coastal water quality and productivity. Geochim. Cosmochim. Acta 69, A760–A760.

Zektser, I.S., Everett, L.G., 2000. Groundwater and the Environment: Applications for the Global Community. CRC Press.

Zemann, J., Craig, P., 2005. Natural history guide to American Samoa. Acta Crystallogr. 18, 139. https://doi.org/10.1107/S0365110X65000361

Zennaro, B.B., 2007. Regulating Illegal Piggery Waste Runoff. http://www.esri.com/news/arcnews/fall07articles/regulating-illegal.html (accessed 2017-1-17)

Zhang, M., Yang, J., Xiao, K., Li, H., Zheng, C., An, A., Zhang, Y., Wang, X., 2017. Nutrient inputs through submarine groundwater discharge in an embayment: A radon investigation in Daya Bay, China. J. Hydrol. 551, 784–792. https://doi.org/10.1016/j.jhydrol.2017.02.036